

AD-A149 725

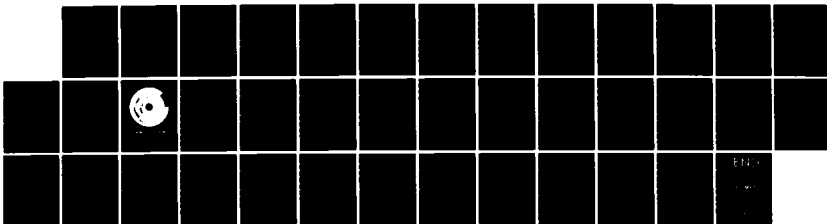
S3-3 ONR-118 DATA ANALYSIS(U) LOCKHEED MISSILES AND
SPACE CO INC PALO ALTO CA PALO ALTO RESEARCH LAB
R D SHARP ET AL. 31 OCT 84 N00014-78-C-0479

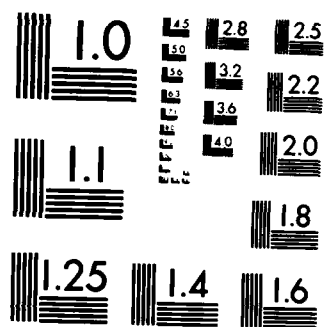
1/1

UNCLASSIFIED

F/G 4/1

NL





MICROCOPY RESOLUTION TEST CHART
NATIONAL BUREAU OF STANDARDS-1963-A

10

AD-A149 725

S3-3 FINAL REPORT
ONR Contract
N00014-78-C-0479

DTIC FILE COPY

DTIC
JAN 30 1985
S E

"Original contains color
plates: All DTIC reproductions
will be in black and
white"

 **Lockheed Missiles & Space Company, Inc.**
SUNNYVALE, CALIFORNIA

This document is approved
for public release
distribution is unlimited

85 01 22 054

REPORT DOCUMENTATION PAGE		READ INSTRUCTIONS BEFORE COMPLETING FORM
1. REPORT NUMBER	2. GOVT ACCESSION NO. AD-A149725	3. RECIPIENT'S CATALOG NUMBER
4. TITLE (and Subtitle) FINAL REPORT S3-3 ONR-118 Data Analysis Contract N00014-78-C-0479		5. TYPE OF REPORT & PERIOD COVERED Final Report for period 6/1/78 - 10/31/84
7. AUTHOR(s) R. D. Sharp, F. G. Shelley, R. G. Johnson, H. L. Collin, A. G. Ghielmetti, J. M. Quinn		6. PERFORMING ORG. REPORT NUMBER
9. PERFORMING ORGANIZATION NAME AND ADDRESS Space Sciences Laboratory, Dept. 91-20, Bldg. 255 Lockheed Palo Alto Research Laboratory 3251 Hanover Street, Palo Alto, CA 94304		8. CONTRACT OR GRANT NUMBER(s) N00014-78-C-0479
11. CONTROLLING OFFICE NAME AND ADDRESS Mr. R. Gracen Joiner, Code 414 Office of Naval Research Arlington, Virginia 22217		10. PROGRAM ELEMENT, PROJECT, TASK AREA & WORK UNIT NUMBERS
14. MONITORING AGENCY NAME & ADDRESS (if different from Controlling Office)		12. REPORT DATE 31 October 1984
		13. NUMBER OF PAGES 35
		15. SECURITY CLASS. (of this report) UNCLASSIFIED
		15a. DECLASSIFICATION DOWNGRADING SCHEDULE
16. DISTRIBUTION STATEMENT (of this Report) Approved for public release; distribution unlimited.		
17. DISTRIBUTION STATEMENT (of the abstract entered in Block 20, if different from Report) Approved for public release; distribution unlimited.		
18. SUPPLEMENTARY NOTES		
19. KEY WORDS (Continue on reverse side if necessary and identify by block number) Auroral processes ion composition, ionosphere-magnetosphere coupling, particle acceleration.		
20. ABSTRACT (Continue on reverse side if necessary and identify by block number) This report describes results of the ONR-118 instrument flown on the S3-3 satellite launched in July 1976 into a near polar orbit with apogee of 8,000 km. The instrument measured ion composition in the energy range $E/Q = 0.5-16$ keV/e, and electron fluxes in four bands between .07-24. keV. (continued on back)		

UNCLASSIFIED

SECURITY CLASSIFICATION OF THIS PAGE(When Data Entered)

Principal results in the period of this contract addressed the acceleration of ionospheric ions and their trapping in the magnetosphere; the observation of narrow electron beams; and the characterization and modeling of auroral processes as manifested by the interactions of particles with the waves and fields of the auroral acceleration region. Energetic ions were observed resulting from both quasistatic electric fields and mass dependent transverse acceleration. Properties of ion outflow were examined as a function of latitude, local time, altitude, magnetic activity, and solar cycle phase. Electron beams were observed closely clustered in latitude with upflowing ions, and with an apparent source location at altitudes at or above $1 R_E$. In the case of counterstreaming electrons, observations implied a source in multiple flickering double layers. The distributions of different ion species have been used in studies of wave growth stability and wave particle interactions, the morphology and dynamics of auroral processes, and the transport processes involved in magnetosphere-ionosphere coupling.

Accession For	
NTIS GRA&I	<input checked="" type="checkbox"/>
DTIC TAB	<input type="checkbox"/>
Unannounced	<input type="checkbox"/>
Justification	
By _____	
Distribution/ _____	
Availability Codes	
Dist	Avail and/or Special
A-1	



Original contains color plates: All DTIC reproductions will be in black and white

UNCLASSIFIED

SECURITY CLASSIFICATION OF THIS PAGE(When Data Entered)

Final Report

S3-3 ONR-118 Data Analysis Contract N00014-78-C-0479

INTRODUCTION

The ONR-118 instrument was launched into a near polar orbit in July 1976 aboard the Air Force satellite S3-3. The instrument's principal function was to measure ion composition in the energy range of $E/Q=0.5-16.0$ keV/e. Three spectrometers were used to determine mass spectra at 12 points over the energy range. In addition, fixed magnetic analyzers measured electron fluxes in four broad energy bands between .07 and 24. keV. Both the ion and electron portions obtained good pitch angle coverage with detector angular resolution of approximately 5 degrees.

Early data immediately indicated that S3-3 was sampling the principal auroral acceleration region. The initial contract for the ONR-118 instrument (N00014-72-C-0234) supported several substantial advances in the knowledge of auroral processes and identified the ionosphere as an important source of energetic plasma in the magnetosphere. Significant results included the direct observation of energetic ions flowing out of the ionosphere; the observation of ionospheric ions in the stormtime ring current; the observation of ions accelerated transverse to the magnetic field; and a morphological study of the distribution in latitude, local time, and altitude of upward flowing energetic ions. These and other initial results from S3-3 provided the impetus for a rapid evolution in the understanding of the auroral acceleration region.

The questions raised by early S3-3 results led to keen interest by the scientific community in the study of numerous physical processes occurring in the regions of space traversed by the S3-3 orbit. As described below, the ONR-118 data analysis contract, N00014-78-C-0479, has supported a continuing improvement

in the understanding of these processes and has allowed an impressive harvest from this unique data set.

RESULTS OF THE ION MASS SPECTROMETER

Following the establishment of the importance of the ionosphere as a source of energetic plasma, work has concentrated on clarifying the mechanisms which energize the cold ionospheric ions and inject them into the magnetospheric plasma. Analysis of pitch angle and energy spectrum signatures has shown that parallel electric fields play a major role. Electron pitch angle structure observed by ONR-118 indicated the existence of an extended, magnetic field-aligned electric field both above and below the spacecraft (Cladis and Sharp, 1979; Sharp et al., 1979). Upward flowing, nearly field-aligned O^+ and H^+ ions were observed to have spectra peaked near the energy corresponding to the electric potential deduced for the region below the spacecraft. However the peaked ion spectra were sufficiently broad to rule out pure electrostatic acceleration. The potential drops deduced from these measurements were of several kilovolts, with vertical extents on the order of 1000 km.

In addition to electrostatic acceleration parallel to the magnetic field, the data show that significant, mass dependent, transverse acceleration also occurs (Collin et al., 1981, Sharp, 1981). In contrast to the field-aligned ions resulting from the effects of parallel electric fields, broad ion conic distributions indicate that transverse acceleration is sometimes dominant. A statistical study of upflowing ion characteristics found that both the average beam energy and pitch angle width of upflowing O^+ were substantially larger than for H^+ . An analysis of electrons observed coincident with upflowing ions determined that the average electron energy was generally between the average

proton energy and the average oxygen energy. This study concluded that while protons receive the bulk of their energy from the parallel electric field, the O^+ ions obtain approximately half of their energy from a mass dependent, transverse acceleration process. Electrons apparently receive substantial energization from the electrostatic field.

The existence of this transverse acceleration is clearly an important factor in the trapping of ionospheric plasma in the plasma sheet population. With purely field-aligned electrostatic acceleration, one would expect to see statistically comparable numbers of downflowing ion beams as upflowing. However, observations by S3-3 (Ghielmetti et al., 1979) found that downflowing ions are much less frequent than upflowing ions. This indicates that the ionospheric ions are commonly trapped in the plasma sheet, and that they may provide a significant fraction of the substorm injected plasma.

The direct ion injection from the ionosphere into the plasma sheet is supplemented by ions which take a more circuitous route. Measurements in the low altitude dayside cusp (Shelley, 1979a) reveal that ionospheric ions are continuously accelerated into the high latitude boundary layers.

Key insights into the variations of ionospheric outflow with magnetic activity were provided by the ONR-118 data set. The data were used to estimate the total high latitude outflow of terrestrial ions during magnetic storms and quiet periods (Collin et al., 1984). While an enhanced outflow was observed for both H^+ and O^+ during magnetic storms, the ratio of O^+/H^+ outflow increased dramatically from 0.25 during quiet times to 1.4 during storms.

The injection of O^+ during a particular storm period was studied using data from both S3-3 and SCATHA (Strangeway and Johnson, 1984). A density enhancement of ionospheric plasma was observed moving to lower L shells as the storm's recovery phase progressed. This apparent movement was explained in terms of time of flight effects in the convection of the injected plasma.

In addition to variations in ionospheric outflow with magnetic activity, it is becoming clear that there are long term variations in auroral ion acceleration processes associated with the solar cycle. The occurrence frequency of upflowing ions within the ONR-118 energy coverage decreased by more than an order of magnitude from late 1977 to early 1979. However, the large fluxes of O^+ observed by SCATHA during 1979 indicate that ionospheric ions were still being accelerated into the trapped population during this time. The most likely reconciliation of these results is that the fundamental acceleration region of ionospheric ions moved above the S3-3 altitude during the solar maximum period.

Complementing the many studies of specific physical phenomena, the ONR-118 data set has also contributed to an evolving synthesis of the overall understanding of auroral and magnetospheric processes. A series of papers (Shelley, 1979b; Johnson, 1983; Sharp et al., 1983; Shelley, 1984) have documented the contributions of the S3-3 energetic ion composition measurements to the continually improving global picture of these processes. The review paper: "Hot Plasma Composition Results from the S3-3 Spacecraft" summarizes the key results of the ion composition portion of ONR-118. A copy of this paper is attached.

RESULTS OF THE ELECTRON DETECTORS

Narrowly collimated, field-aligned, counterstreaming electron beams were observed to occur at altitudes between 4000 and 8000 km (Sharp et al., 1980). These electron beams were composed of intense fluxes with energies in the keV range, with angular widths as narrow as 1 degree. The energy spectra were broad and the loss cones of precipitating plasma sheet electrons were most often unaffected. The data cannot be explained in terms of acceleration by a simple quasistatic electric field. A model proposed for the generation of these beams

involved the acceleration of cold ambient plasma by multiple flickering double layers.

A statistical study of electron beams in the polar regions (Collin et al., 1982) found a good correlation between the beams and the statistical auroral oval. The beams were found to be clustered closely in latitude with upward flowing ions, with the mean electron beam latitude slightly equatorward of the mean upward flowing ion position. The beams were usually not observed at energies above 400 eV. The altitude distribution of the beams indicated a source region at or above an altitude of 1 RE. The results of the statistical study also suggested a multiple flickering double layer source.

An analysis of the relationship of both trapped and precipitating electrons to upflowing ions yielded several important results (Collin et al., 1981). The average energy of electrons observed in the presence of upflowing ions was found to typically lie between that of the protons and oxygen. A good correlation was found between the energies of upflowing oxygen ions and locally mirroring electrons. The average electron spectra were broadly peaked, with the peak energy increasing with increasing energy of the associated upward flowing oxygen.

COOPERATIVE STUDIES USING ONR-118 DATA

The ONR-118 data have been shared cooperatively in a number of projects. These projects have combined data from several instruments in order to obtain a more complete observational picture and to provide sensitive tests of theoretical models.

Ion composition data have provided valuable contributions to the investigation of wave-particle interactions in the auroral acceleration region

(Kauffman and Kintner, 1982; Kintner et al., 1979). The analyses have concentrated on the stability of electrostatic ion cyclotron waves and the causal relationship behind the close correlation of upward flowing ions and the waves. The stability of ion ring distributions in the cusp was also studied with respect to the generation of lower hybrid waves and the subsequent heating of different ion species (Roth and Hudson, 1984).

Another area of cooperative effort has been the exploration of the overall morphology and dynamics of the auroral acceleration region. Studies have dealt with auroral particle acceleration processes acting on both electrons and ions (Mozer et al., 1980), the structure of strong electric field regions and their relationship to particle acceleration (Mizera et al., 1981b; Temerin et al., 1981), and auroral morphology (Mizera et al., 1981a)

S3-3 ion and electron measurements have played an important role in the understanding of magnetosphere-ionosphere coupling (Kaufmann and Kintner, 1984; Kaufmann, 1984). In particular, ions were found to carry the majority of field-aligned momentum flux, while electrons carry currents. Ion composition information is critical to the analysis of momentum balance within the acceleration region.

Papers published with support from N00014-78-C-0479

Cladis, J.B. and R.D. Sharp, Scale of Electric Field Along Magnetic Field in an Inverted V Event, J. Geophys. Res., 84, p. 6564, 1979.

Collin, H.L., R.D. Sharp, E.G. Shelley, and R.G. Johnson, Some General Characteristics of Upflowing Ion Beams Over the Auroral Zone and Their Relationship to Auroral Electrons, J. Geophys. Res., 86, p. 6820, 1981.

Collin, H.L., R.D. Sharp, and E.G. Shelley, The Occurrence and Characteristics of Electron Beams Over the Polar Regions, J. Geophys. Res., 87, p. 7504, 1982.

Collin, H.L., R.D. Sharp, and E.G. Shelley, The Magnitude and Composition of the Outflow of Energetic Ions from the Ionosphere, J. Geophys. Res., 89, p. 2185, 1984.

Ghielmetti, A.G., R.D. Sharp, E.G. Shelley, and R.G. Johnson, Downward Flowing Ions and Evidence for Injection of Ionospheric Ions Into the Plasma Sheet, J. Geophys. Res., 84, p. 5781, 1979.

Johnson, R.G., The Hot Ion Composition, Energy, and Pitch Angle Characteristics Above the Auroral Zone Ionosphere, in High-Latitude Space Plasma Physics, Ed. B. Hultqvist and T. Hagfors, Plenum Publishing, p. 271, 1983.

Kaufmann, R.L. and P.M. Kintner, Upgoing Ion Beams 1: Microscopic Analysis, J. Geophys. Res., 87, p. 10487, 1982.

Kaufmann, R.L. and P.M. Kintner, Upgoing Ion Beams 2: Fluid Analysis and Magnetosphere-Ionosphere Coupling, J. Geophys. Res., 89, p. 2195, 1984.

Kaufmann, R.L., What Auroral Electron and Ion Beams Tell Us About Magnetosphere-Ionosphere Coupling, Space Sci. Rev., in press, 1984.

Kintner, P.M., M.C. Kelley, R.D. Sharp, A.G. Ghielmetti, M. Temerin, C. Cattell, P.F. Mizera, and J.F. Fennel, Simultaneous Observations of Energetic (keV) Upstreaming and Electrostatic Hydrogen Cyclotron Waves, J. Geophys. Res., 84, p. 7201, 1979.

Mizera, P.F., J.F. Fennel, D.R. Croley, A.L. Vampola, F.S. Mozer, R.B. Torbert, M. Temerin, R. Lysak, M. Hudson, C.A. Cattell, R.J. Johnson, R.D. Sharp, A. Ghielmetti, and P.M. Kintner, The Aurora Inferred From S3-3 Particles and Fields, J. Geophys. Res., 86, p. 2329, 1981a.

Mizera, P.F., J.F. Fennel, D.R. Croley, and D.J. Gorney, Charged Particle Distributions and Electric Field Measurements From S3-3, J. Geophys. Res., 86, p. 7566, 1981b.

Mozer, F.S., C.A. Cattell, M.K. Hudson, R.L. Lysak, M. Temerin, and R.B. Torbert, Satellite Measurements and Theories of Low Altitude Auroral Particle Acceleration, Space Sci. Rev., 27, p. 155, 1980.

Roth, I., and M. K. Hudson, Lower Hybrid Heating of Ionospheric Ions Due to Ion Ring Distributions in the Cusp, submitted to J. Geophys. Res., 1984.

Sharp, R.D., R.G. Johnson, and E.G. Shelley, Energetic Particle Measurements From Within Ionospheric Structures Responsible for Auroral Acceleration Processes, J. Geophys. Res., 84, p. 480, 1979.

Sharp, R.D., E.G. Shelley, R.G. Johnson, and A.G. Ghielmetti, Counterstreaming Electron Beams at Altitudes of 1RE Over the Auroral Zone, J. Geophys. Res., 85, p. 92, 1980.

Sharp, R.D., Positive Ion Acceleration in the 1 RE Altitude Range, in The Physics of Auroral Arc Formation, ed. S.I. Akasofu and J.R. Kan, Geophysical Monograph 25, American Geophysical Union, p. 112, 1981.

Sharp, R.D., A.G. Ghielmetti, R.G. Johnson, and E.G. Shelley, Hot Plasma Composition Results from the S3-3 Spacecraft, p. 167, in Energetic Ion Composition in the Earth's Magnetosphere, ed. R.G. Johnson, Terra Scientific Publishing, 1983.

Sharp, R.D., W. Lennartsson, and R.J. Strangeway, The Ionospheric Contribution to the Plasma Environment in Near-Earth Space, submitted to Radio Science, 1984.

Shelley, E.G., Ion Composition in the Dayside Cusp: Injection of Ionospheric Ions Into the High Latitude Boundary Layer, in Proceedings of Magnetospheric Boundary Layers Conference, Alpbach, ESA SP-148, 1979a.

Shelley, E.G., Heavy Ions in the Magnetosphere, Space Sci. Rev., 23, p. 465, 1979b.

Shelley, E.G., Circulation of Energetic Ions of Terrestrial Origin in the Magnetosphere, Advances in Space Res., submitted 1984.

Strangeway, R.J. and R.G. Johnson, Energetic Ion Mass Composition as Observed at Near Geosynchronous and Low Altitudes During the Storm Period of February 21 and 22, 1979, J. Geophys. Res., 89, p. 8919, 1984.

Temerin, M., C. Cattell, R. Lysak, M. Hudson, R.B. Torbert, F.S. Mozer, R.D. Sharp, and P.M. Kinter, The Small-Scale Structure of Electrostatic Shocks, J. Geophys. Res., 86, p. 11278, 1981.

Hot Plasma Composition Results from the S3-3 Spacecraft

R. D. SHARP, A. G. GHIEMMETTI, R. G. JOHNSON, and E. G. SHELLEY

*Space Sciences Laboratory, Lockheed Palo Alto Research Laboratory,
3251 Hanover Street, Palo Alto, California, U.S.A.*

(Received March 26, 1982)

The S3-3 satellite discovered the principal auroral acceleration region at altitudes of about $1 R_E$ over the auroral zone. Intense fluxes of upward flowing O^+ and H^+ ions with keV energies were commonly observed in this region of the magnetosphere. The detailed morphology of these upflowing ions is described, including their latitude, local time, altitude, and magnetic activity dependences and their relationship to the trapped keV electron population. The first measurements of the composition of the trapped keV ions in the radiation belts are also described, showing the importance of the ionospheric source term to the storm time population of ions with energies ≤ 16 keV/e.

1. Introduction

Beginning in about 1970, certain characteristics of the distribution functions of the precipitating auroral electrons began to be interpreted as evidence that an electrostatic acceleration process was acting to energize them (GURNETT, 1972; EVANS, 1975). Satellite measurements were unable to provide any direct confirmation of these inferences because the satellites were generally limited to low altitude polar or geostationary orbits, outside the region where the acceleration process occurs. In July 1976 the Air Force satellite S3-3 with a modest payload of energetic particle and field detectors was placed into a near polar orbit with an apogee of $\sim 8,000$ km. It immediately became clear that at that altitude it was encountering the region where the principal auroral acceleration mechanisms were operative (SHELLEY *et al.*, 1976; SHARP *et al.*, 1977b). Direct measurements of electric field intensities of up to several hundred millivolts/meter were provided by the U. C. Berkeley experiment (MOZER *et al.*, 1979). Signatures of in situ acceleration processes were found with the particle detectors (MIZERA and FENNELL, 1977; SHARP *et al.*, 1979). The directions of the inferred electrostatic potentials were such that they energized electrons in the downward direction and precipitated them into the atmosphere while simultaneously accelerating ambient ionospheric ions upward, injecting them into the radiation belts. The relative scarcity of observations of downward flowing ions in the altitude range of S3-3 suggested that this injection process was quite efficient (GHIEMMETTI *et al.*, 1979).

The Lockheed experiment on S3-3 contained an energetic ion mass spectrometer and provided the added dimension of ion composition information to the understanding of the complex plasma processes operative in this region. These

measurements have provided useful information in three principal areas:

1. The study of the detailed characteristics of the several acceleration mechanisms found to be operative in the 4,000–8,000 km altitude region on auroral field lines.
2. The definition of the morphology of the upward flowing energetic ions which are the principal source term for that portion of the magnetospheric particle population which is of ionospheric origin.
3. The composition of the stormtime ring current. S3-3 provided the first direct measurements of the ion composition of this population of particles (JOHNSON *et al.*, 1977).

In this review we shall examine the role of the ion composition data in understanding the magnetospheric processes operating in each of these three areas.

The S3-3 ion mass spectrometer experiment contained three individual sensors, each of which covered a separate portion of the energy per unit charge range from 0.5 to 16 keV/e. The sensors were mounted with their view directions perpendicular to the spacecraft spin axis so that they obtained a complete angular scan at three energies approximately every 20 sec. A 12 point energy spectrum of ions with mass per charge from 1 through 32 was acquired every 64 sec. A more complete description of the experiment is contained in SHARP *et al.* (1977b).

2. Ion Acceleration Mechanisms

These results have recently been reviewed (SHARP, 1981) and we will present here only a brief summary of the principal conclusions to this time.

Upward flowing H^+ and O^+ ions with energies in the keV range were frequently observed on auroral field lines by S3-3 at altitudes above 4,000 km. He^+ ions were also observed but substantially less frequently and with much lower intensity than H^+ and O^+ . The upward flowing ions were often found in association with the signatures of parallel electric fields in the keV electron distributions. These signatures on occasions allowed a quantitative estimate to be made of an electrostatic potential difference below the spacecraft, and in a number of cases when direct comparisons were made this potential was found to correspond approximately to the energy at which the upflowing ions exhibited a peak in their energy spectrums (CLADIS and SHARP, 1979; MIZERA *et al.*, 1981). This implies that a large fraction of the ion energy was acquired electrostatically. The spectral peaks were quite broad, however, and the angular distributions of the upflowing ion beams were typically wider than would be expected if the beams resulted from a pure electrostatic acceleration of the ambient thermal plasma. Also, upon occasions the upflowing ions exhibited a "conical" pitch angle distribution (with a local minimum in the distribution along the direction of the magnetic field). These characteristics implied that some transverse acceleration mechanism was also involved in the energization process.

Statistical results, which will be discussed below in more detail, showed that the energy of the O^+ beams was typically $1\frac{1}{2}$ to 2 times that of the H^+ , and their angular widths were substantially broader. The median value of the half widths was 24° for the O^+ beams and 15° for the H^+ (COLLIN *et al.*, 1981). If we further consider that the

upflowing ion beams (with $E > 0.5$ keV) are only found at altitudes above about 4,000 km (GHIELMETTI *et al.*, 1978), these parameters allow us to set limits on the relative strengths of the transverse and parallel ion acceleration mechanisms. It was concluded by COLLIN *et al.* (1981) that the H^+ ion beams could typically only receive a small fraction of their energy from a transverse acceleration mechanism acting above 4,000 km or they would have angular widths larger than those observed. The O^+ ions on the other hand could derive almost half of their energy from such a mechanism. These results were taken to imply that:

1. The H^+ ions were accelerated primarily by parallel electric fields.
2. The O^+ received on the average the same parallel acceleration as did the H^+ .
3. The excess energy in the O^+ relative to the H^+ was provided by some transverse acceleration mechanism that preferentially acted on the O^+ constituent of the ion beams.

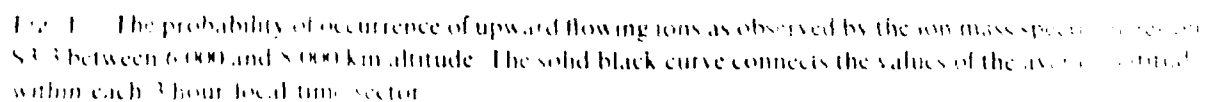
Some of the other results of these statistical studies which are relevant to our understanding of the properties of the ion acceleration mechanism as well as to the characterization of the ionospheric source term for the ring current are discussed in Section 4.

3. Morphology of Upward Flowing Ions

Some of the results of a study of the characteristics of the upward flowing ion events were reported by GHIELMETTI (1978), GHIELMETTI *et al.* (1978), and SHELLEY *et al.* (1980). The data which were utilized were acquired during the period July 13, 1976 to September 27, 1977, and included 925 orbits covering the complete range of local time. Because of the phasing of the orbit with season, almost all of the data were acquired over the summer hemisphere. The polar regions between 60 and 84 degrees invariant latitude (ILA) were subdivided into unit bins of size 2° ILA by three hours magnetic local time (MLT) by 1,000 km altitude. A bin was defined to have been sampled if at least one complete pitch angle scan was acquired while the satellite passed through it. An upward flowing ion (UFI) event was defined as the occurrence of at least one observation within a unit bin of an anisotropic pitch angle distribution with a maximum in the upward moving direction. Additionally it was required that the flux exceed the sensitivity threshold of $\sim 2 \times 10^6$ keV/(cm² sec ster keV) and also exceed the penetrating energetic electron background.

The probability of occurrence was defined as the ratio of the number of UFI events to the number of samples. For this analysis no distinction was made between field aligned distributions (beams) and conical events but the latter were relatively rare in this energy range and so the results are generally representative of field aligned events. For each event, in addition to the occurrence probability, the following parameters were recorded for the two most commonly observed ion species (H^+ and O^+): The peak differential energy flux, the energy at the peak flux, the maximum energy at which upflowing ions were observed, the magnetic local time, the invariant latitude, the altitude, and K_p . A total of about 19,397 samples were obtained in the period of this analysis and about 936 upward flowing ion events were observed.

Figure 1 shows a principal result of the study, a magnetic local time, invariant



latitude map of the probability of occurrence of upward flowing ions observed between 6,000 and 8,000 km altitude within the energy and sensitivity ranges defined above. The solid black curve connects the values of the average latitude within each local time sector. The white area in the 06–09 hour sector was deleted because it was not adequately sampled. The principal features of this distribution, the dramatic maximum in local evening and the general correspondence to the auroral oval, are in agreement

with the previous less detailed results derived from the more limited data set published earlier (GHIEMMETTI *et al.*, 1978).

3.1 Local time dependence

The local time asymmetry in the probability of occurrence is more strikingly evident in Fig. 2 which was obtained from the results in Fig. 1 by summing over the latitudinal distributions within each three hour local time sector. The error bars in this and subsequent figures represent the standard deviations of the means of the probability distributions. In order to investigate the dependence of this distribution on magnetic storm activity the data were subdivided into "disturbed" periods, during the initial phase or early recovery phase of magnetic storms, and "quiet" periods which had relatively low *Dst* and were at least several days after the recovery phase of the last previous magnetic storm. These results are shown in Figure 3. One sees that there is only a modest increase in occurrence probability during the storms and no qualitative difference in the pattern between disturbed and quiet times.

The local time dependence of the energy of the upflowing ions was investigated by forming the average of the energies at which the peak energy flux was recorded for each event. These results are illustrated in Figure 4. One sees a strong dependence on local time with the hardest events being observed in the premidnight sector. The O^+ is seen to be substantially harder than the H^+ . A rough indication of the energy width of the ion distribution functions is also illustrated for the O^+ events by the dashed curve in Figure 4. This is the average of the maximum energies at which flux was observable on each event.

The ion composition was also observed to have a significant local time dependence. Figure 5 shows the ratio of the occurrence frequencies of O^+ and H^+ events

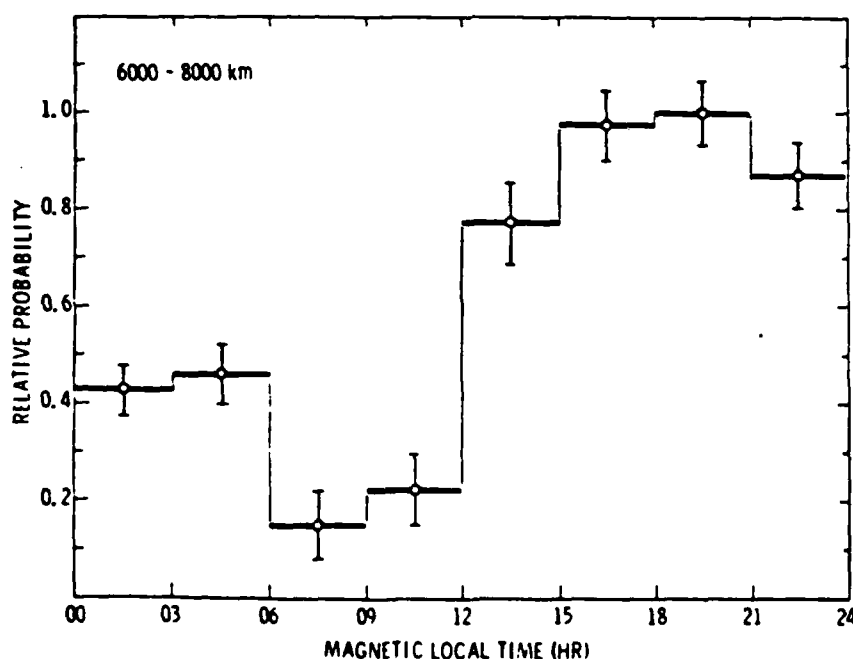


Fig. 2. Relative probability of occurrence of upward flowing ions as a function of magnetic local time.

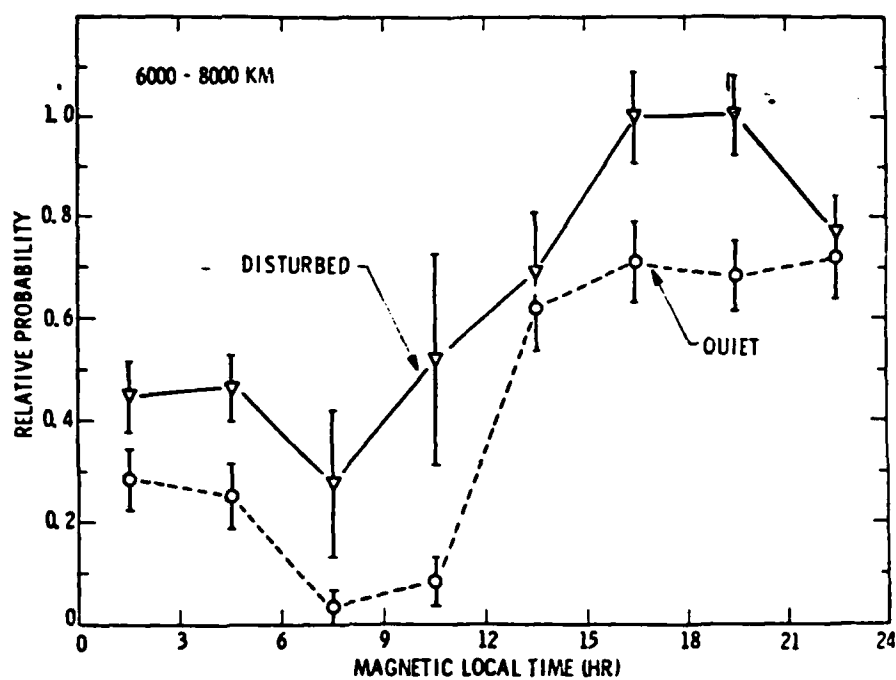


Fig. 3. A comparison of the probabilities of upward flowing ions between quiet and disturbed periods.

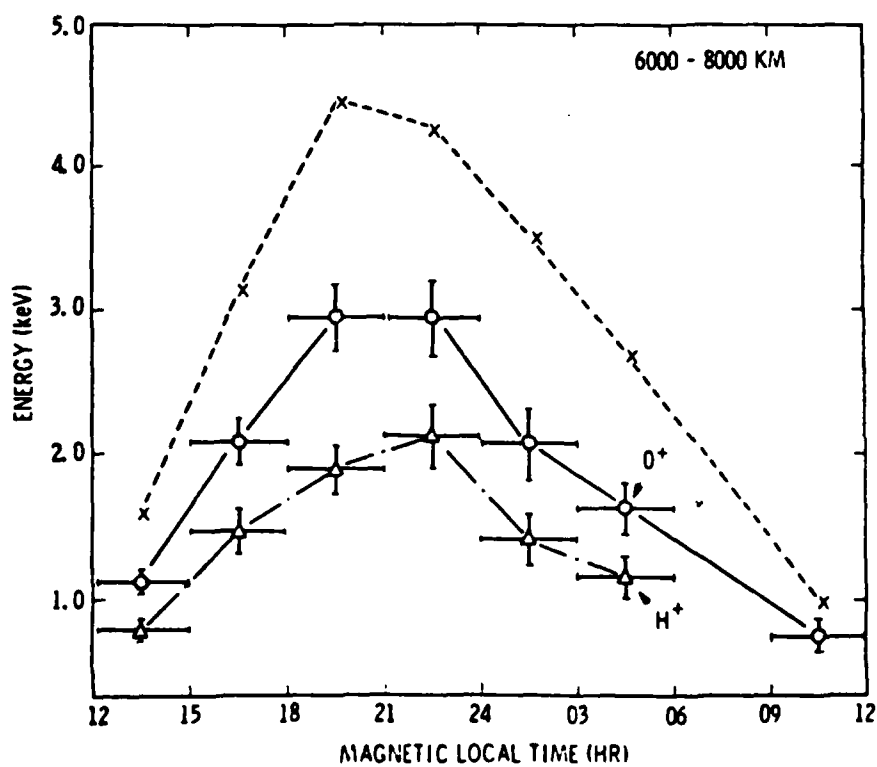


Fig. 4. Average of the energies at which the peak energy flux was observed as a function of magnetic local time (circles represent O⁺ and triangles represent H⁺) and average of the maximum energies at which O⁺ flux was observed (crosses).

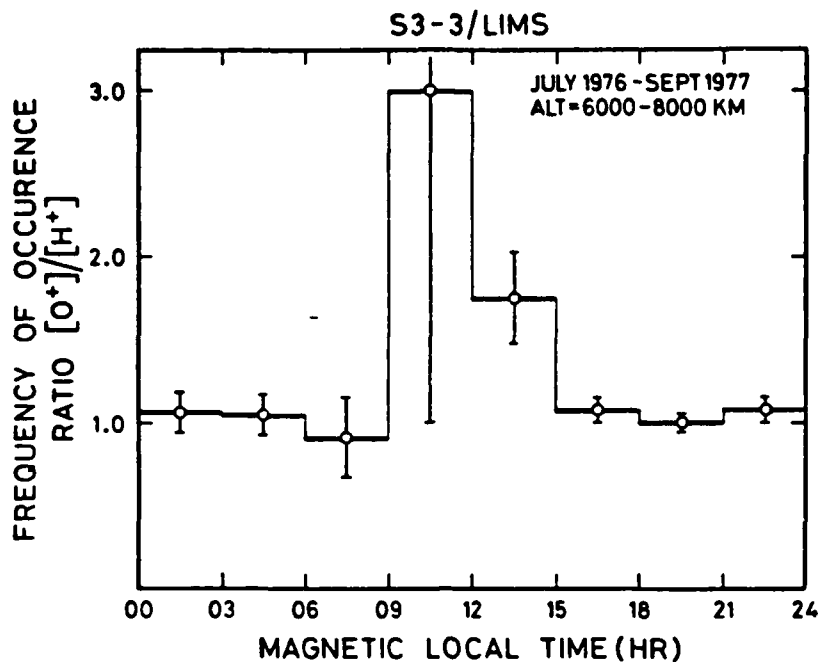


Fig. 5. Ratio of the occurrence frequencies of O^+ and H^+ events as a function of magnetic local time.

as a function of magnetic local time. One sees a dramatic change in composition in the vicinity of local noon associated with the acceleration of ionospheric O^+ ions in the dayside cusp (SHARP *et al.*, 1977b; SHELLEY, 1979). As will be discussed below, this acceleration acts most frequently on the transverse component of the O^+ ion energy, leading to the observation of conical pitch angle distributions. The plot shown in Figure 5 should be considered only as a qualitative indicator of the composition in the region of the cusp since it is quite difficult to identify transversely accelerated ionospheric H^+ ions in the presence of the intense fluxes of precipitating and magnetically reflecting H^+ ions of solar origin that are present on the cusp field lines. It does serve to characterize the ionospheric acceleration region associated with the cusp as qualitatively different from that in other sectors, in agreement with the results of the morphological studies of GORNEY *et al.* (1981).

3.2 Altitude dependence

Since the local time distributions exhibited a broad flat maximum over the 15–24 hour sector this subset of the data were utilized to study the altitude dependence. For each three hour local time sector the averaged occurrence probabilities in 1,000 km altitudinal bins were formed from sums over the latitude range within which 90% of the events occurred. This altitude distribution is shown in the left panel of Figure 6. In the absence of strong angular diffusion each upflowing beam should be observable at any altitude above its point of origin and the differential of this curve should characterize the location of the source region. This was obtained by subtracting probabilities in adjacent altitude bins and is shown in the right panel of Figure 6. These plots show that ion acceleration to energies above 500 eV occurs primarily at altitudes greater than 4,000 km and also suggests that we may in fact have gone over the peak of the

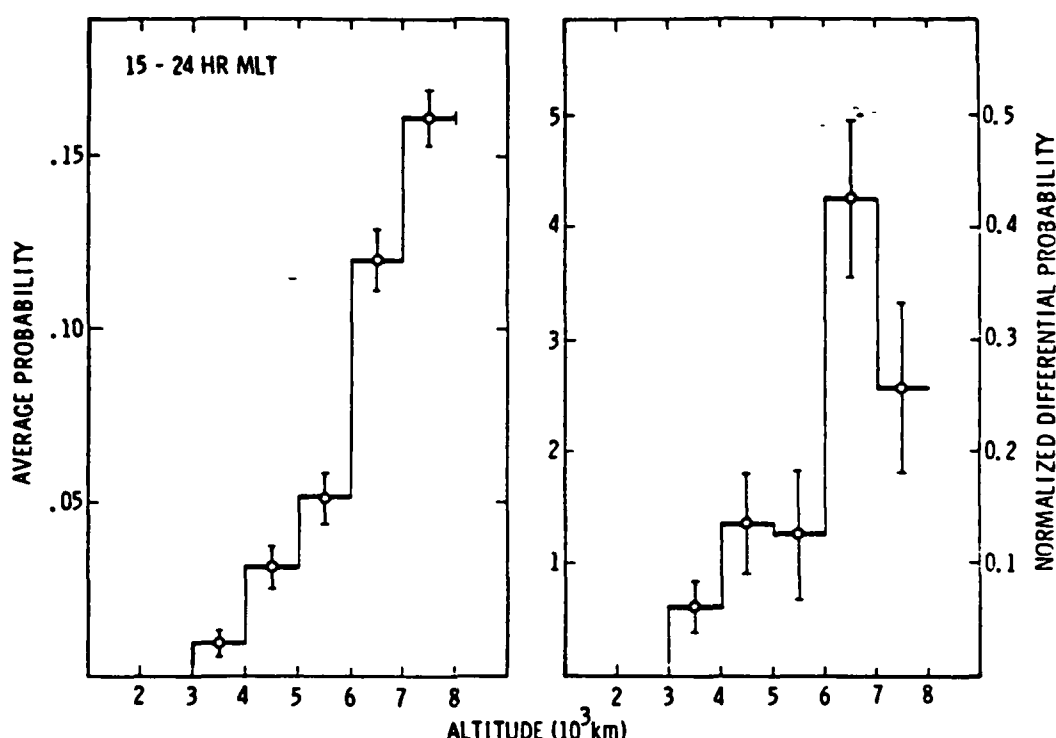


Fig. 6. Left panel: Average occurrence probability per 1,000 km altitude bin in the 15–24 hour magnetic local time sector. Right panel: Normalized differential probability obtained by subtracting probabilities in adjacent altitude bins.

differential altitude distribution at $\sim 6,000$ km. In consideration of the statistical uncertainties, however, the latter result cannot be considered conclusive.

The altitude dependence of the average of the energies at which the peak ion flux was observed is shown by the solid curves in Figure 7. Since the ions receive a substantial fraction of their energy from an electrostatic acceleration mechanism, this quantity should be related to the average electrostatic potential difference in this altitude and local time range. As discussed in Section 2 however, it is apparent from the mass and angular dependencies of the accelerated ions that other mechanisms besides electrostatic acceleration are operative. In view of the statistical uncertainties, no significance is attached to the "peak" at 5,000–6,000 km in the O^+ distribution. The dashed curves represent the averages of the maximum energies at which flux was detectable in each event and again give a rough measure of the energy widths of the ion distributions.

It is significant that at the lowest altitude of observation the ion energy at the peak flux intensity is substantially above the 500 eV energy threshold of the spectrometer and is comparable to the ion energy observed at the highest altitudes. This suggests that on average the acceleration process is nonlinear in altitude and that a substantial energization occurs in a relatively narrow range of altitude near 4,000 km.

The altitude dependence of the ratio of the O^+ to H^+ occurrence probabilities is shown in Figure 8. Within the rather large statistical uncertainties, the results do not show any evidence for an altitude dependence of this ratio and therefore support the

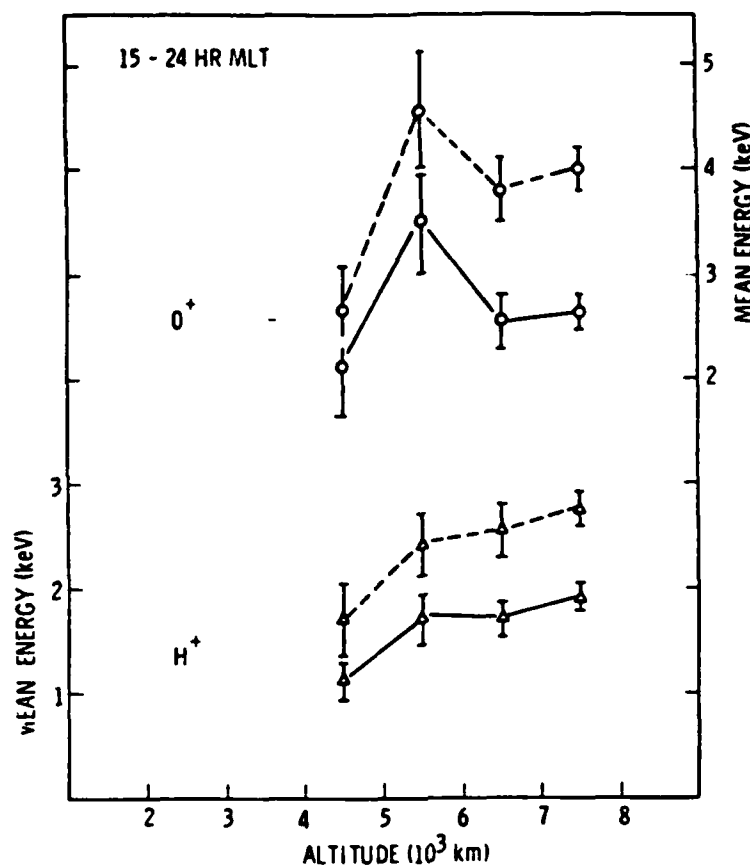


Fig. 7. Average of the energies at which peak flux was observed (solid curves) and average of the maximum energy at which flux was observed (dashed curves). Circles represent O^+ and triangles represent H^+ .

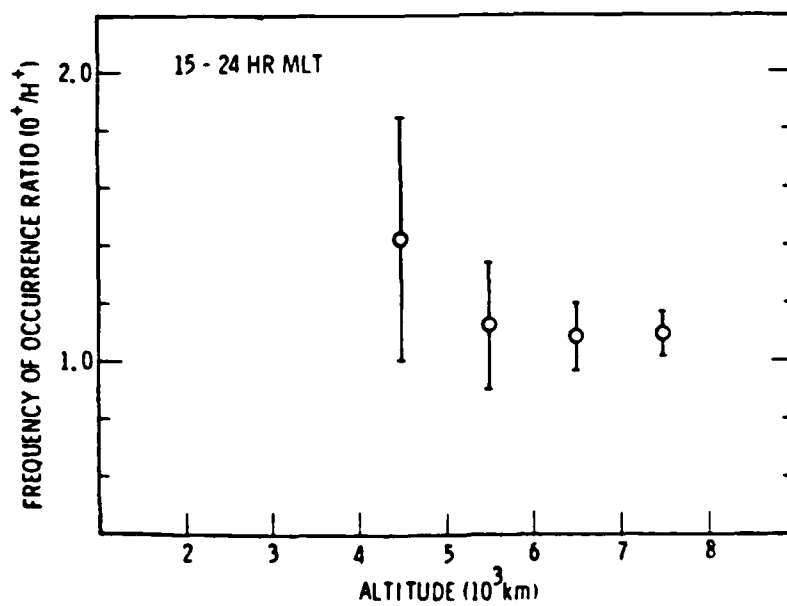


Fig. 8. Ratio of the occurrence frequencies of O^+ and H^+ events as a function of altitude.

inference by COLLIN *et al.* (1981) that the excess energy carried by the O^+ ions did not result from their having entered the acceleration region at systematically lower altitudes than did the H^+ .

3.3 K_p dependence

The distribution of K_p for the data base utilized for this study is shown in Figure 9. Note that reasonable sampling was acquired for $K_p \leq 5$. The K_p dependence of the frequency of occurrence is illustrated in Figure 10, for the O^+ and H^+ separately, for

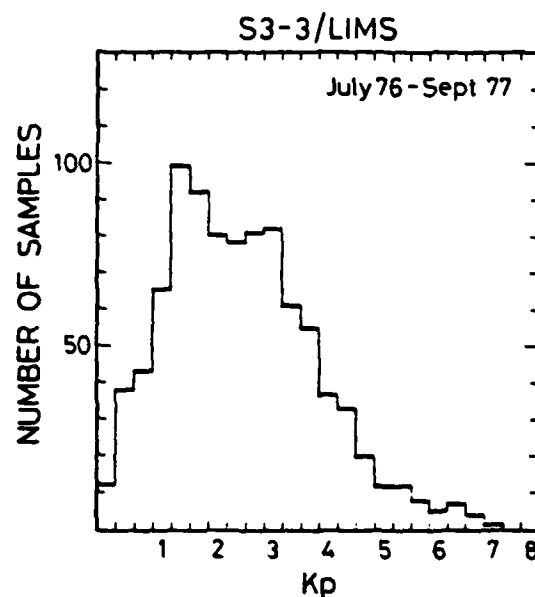


Fig. 9. Distribution of K_p for the data base utilized for this study.

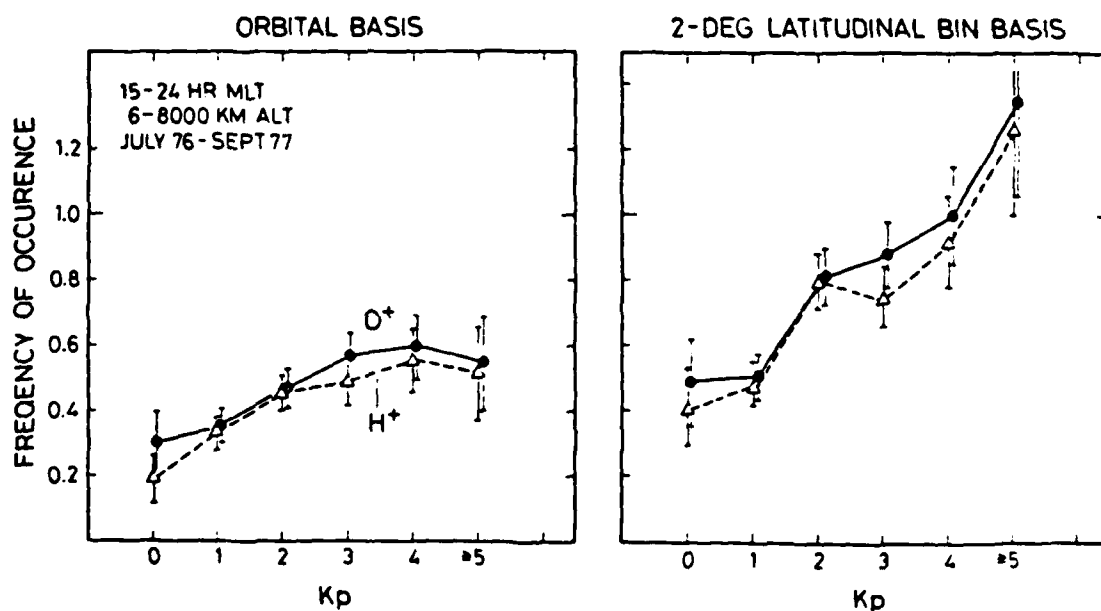


Fig. 10. Frequency of occurrence of O^+ events (circles) and H^+ events (triangles) as a function of K_p . See text for definitions of the two types of frequencies.

events between 15 and 24 hours magnetic local time and with altitudes between 6,000 and 8,000 km. In the left panel the frequency of occurrence is defined on an orbital basis as the number of orbits in which at least one event was observed, divided by the total number of orbits in that K_p range. In the right panel it is defined as the number of 2 degree latitudinal bins in which at least one event was observed divided by the total number of orbits in that K_p range. Note that the latter definition allows frequency of occurrence values greater than 1. The ratio of these two occurrence frequencies gives a rough indication of the latitudinal extent of the UFI region as a function of magnetic activity. An examination of Figure 10 shows that the orbital frequency of occurrence increases from about 25% to about 50% as K_p increases from 0 to 5. The ratio of the two curves (two degree/orbital) ranges from about 1.5 to 2.3 with a small but not clearly significant increase with increasing K_p . An important result is that the H^+ and O^+ ions behave almost identically, with no apparent changes with magnetic activity in the composition as defined by the peak differential energy fluxes.

In order to investigate the relative flux intensities of O^+ and H^+ and their dependence on magnetic activity, the data were organized as follows. Within each range of K_p , the peak energy flux values were arranged according to the energy at which they occurred, and then averaged. This resulted in a set of curves of the type shown in Figure 11. These distributions have the units of a differential flux but should not be confused with such. The curve shown in Figure 11 is the grand average of all of the individual curves in the various K_p ranges and gives a synoptic picture of the energy and mass dependence of the peak flux intensity resulting from the still poorly understood acceleration mechanism responsible for the upward flowing ion fluxes. To illustrate the

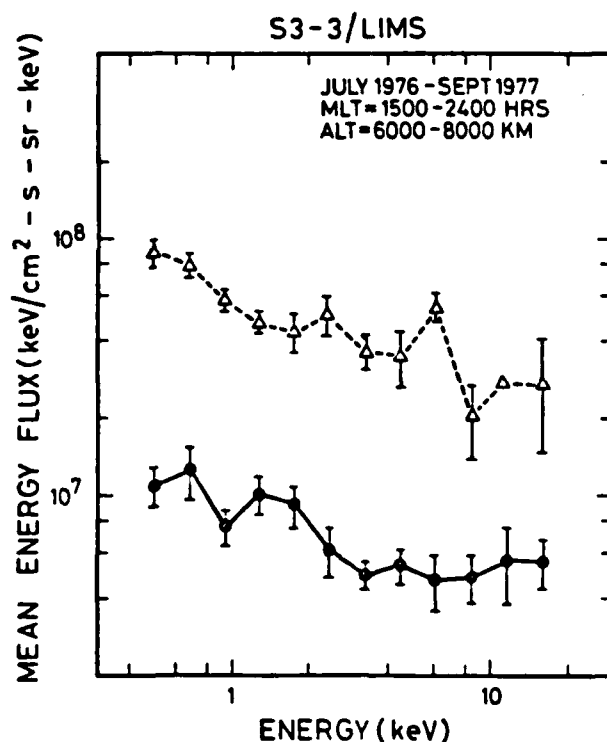


Fig. 11. Averages of peak energy fluxes as a function of energy for O^+ events (circles) and H^+ events (triangles).

K_p dependence of the relative peak fluxes of O^+ and H^+ , the individual curves of the type shown in Figure 11 at each K_p level were integrated over energy to provide a parameter with the units of energy flux. The variation of this parameter with K_p is shown in Figure 12. Again one should note that this is not a true energy flux but the integral of a peak flux distribution. We note that there is no substantial dependence of this parameter on magnetic activity. The corresponding number flux data are shown in Figure 13 where the ratios of the averages of the peak flux integrals for H^+ and O^+ are plotted.

Figure 14 shows two sets of curves computed in a similar manner illustrating the K_p dependence of the mean energy at which the peak flux intensity was observed (lower panel) and the mean of the maximum energies at which a significant flux was observed (upper panel). Here we see an increase with magnetic activity but no significant

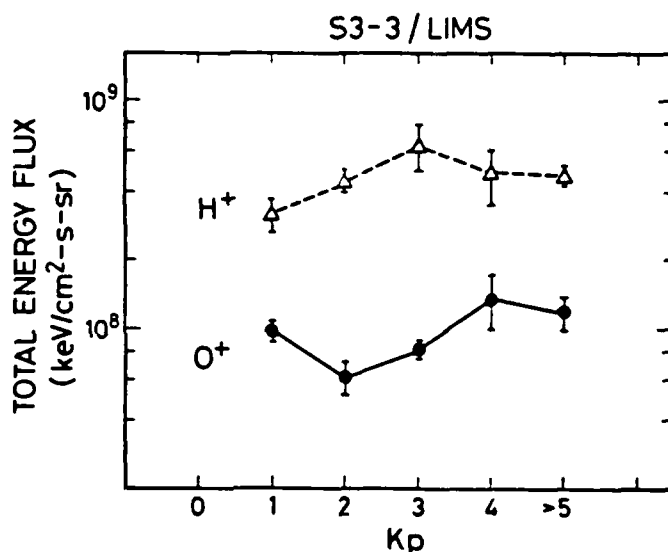


Fig. 12. Integrals of curves of the type shown in Figure 11 as a function of K_p for O^+ events (circles) and H^+ events (triangles).

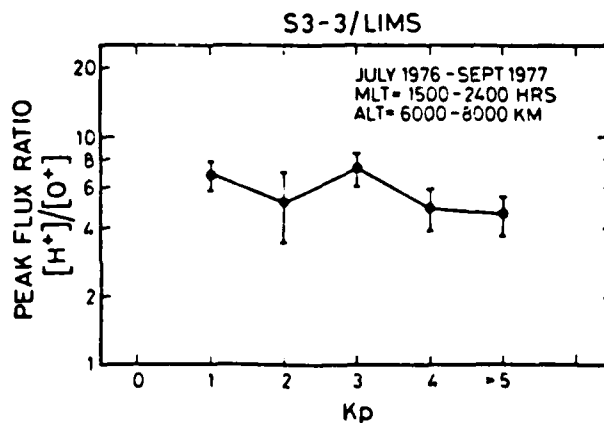


Fig. 13. Number flux data corresponding to the energy flux data presented in Figure 12, shown in the form of the ratios of the peak flux integrals for H^+ and O^+ .

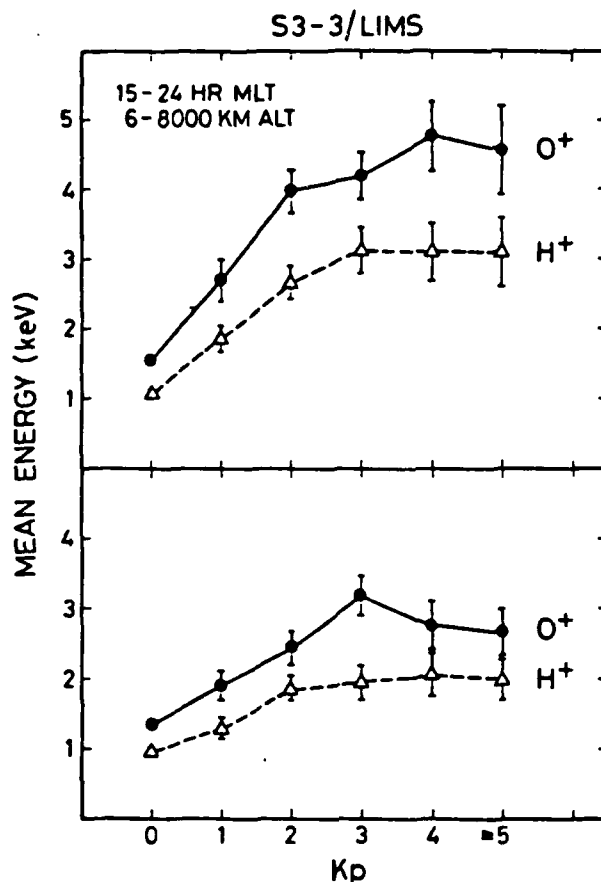


Fig. 14. Mean value of the energy at peak flux intensity (lower panel) and mean value of the maximum energy at which flux was observed (upper panel) as a function of K_p .

difference in the K_p dependence of O^+ and H^+ . This latter result is shown more explicitly in Figure 15 which gives the O^+ to H^+ average energy ratios as a function of K_p . The values represented by the solid dots were formed from the curves in the lower panel of Figure 14 while the values represented by the open triangles were formed from the curves in the upper panel.

3.4 Additional studies

A further study of some of the characteristics of the upward flowing ions beams and their relationship to auroral electrons was conducted by COLLIN *et al.* (1981). This study was based on 44 passes through the upflowing ion regions in the 1800-2400 hour local time sector at altitudes above 6,000 km. In order to focus on a single phenomena, a few wide "conics" (i.e. the events in Figure 19 with widths greater than 50°) were deleted from the remainder of the study. A possibly significant difference between this and the above described study was that COLLIN *et al.* computed the integrated number flux and flux weighted average energy from the peak spectrometer response at each of the 3 measured energies on each spin, rather than utilizing just the flux at the peak energy. Figure 16 shows the frequency of occurrence of upflowing H^+ and O^+ ions as a function of flux intensity. One sees that the maximum H^+ flux was

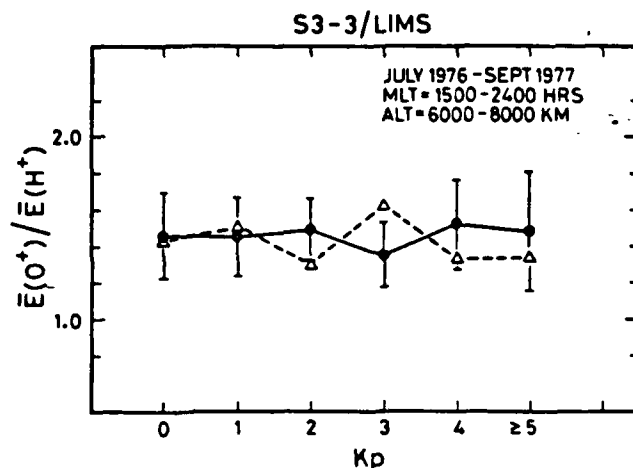


Fig. 15. Ratio of O^+ energy to H^+ energy for the curves in Figure 14. Solid circles represent energy at peak flux intensity and open triangles represent maximum energy at which flux was observed.

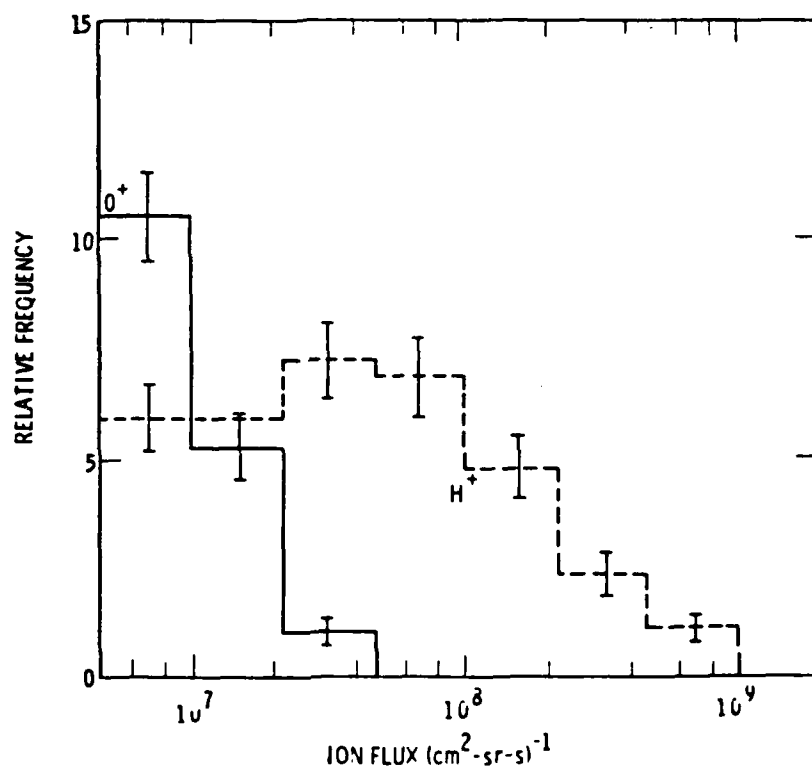


Fig. 16. Occurrence frequency distribution for upflowing O^+ and H^+ ions as a function of flux intensity. Error bars represent statistical uncertainties (COLLIN *et al.*, 1981).

about 20 times as intense as the maximum O^+ flux. The median value of the ratio of H^+ / O^+ intensity was about 7 and no correlation between the flux intensities of the two species was observed.

Both species of ions were observed with energies throughout the range of the instrument. Figure 17 shows the distribution of frequency of occurrence of average energies. The oxygen ions are seen to be significantly more energetic than the protons in

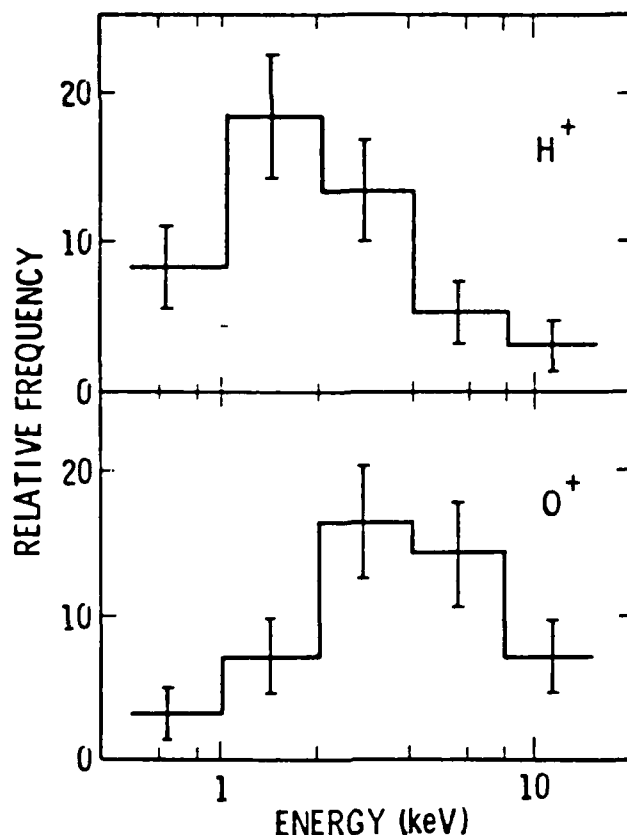


Fig. 17. Occurrence frequency distribution for upflowing O^+ and H^+ ions as a function of average energy (COLLIN *et al.*, 1981).

agreement with the results from the earlier study. The distributions imply that the energy range of the experiment was adequate to characterize the energy range of the ion acceleration mechanism.

Figure 18 shows that there is a clear systematic association between the energies of the two species. The oxygen energy was on the average 1.7 times as great as the proton energy, and the ratio between them ranged from about 0.8 to 3.

The events entering this study were nominally classified as ion "beams" since, as indicated above, the few broad "conics" which appeared to be qualitatively different in character from the majority of the events were deleted from the study. A close examination of the pitch angle distributions showed however that in about 45% of cases for O^+ and 20% of cases for H^+ the pitch angle distributions appeared to have a minimum at the angle of closest approach to the field line. In many of these cases the minimum was close to the limit of statistical significance. The remainder did not show a field-aligned minimum, but in many of these cases the possibility that such a minimum existed could not be ruled out because of the poor counting statistics and because the spectrometers did not always sample closer than 10° to the field line. An estimate of the half width of each distribution was made by finding the pitch angle at which the count rate had dropped to half its maximum observed value. Their occurrence probabilities (Figure 19) show that O^+ had significantly wider pitch angle distributions than H^+ . As

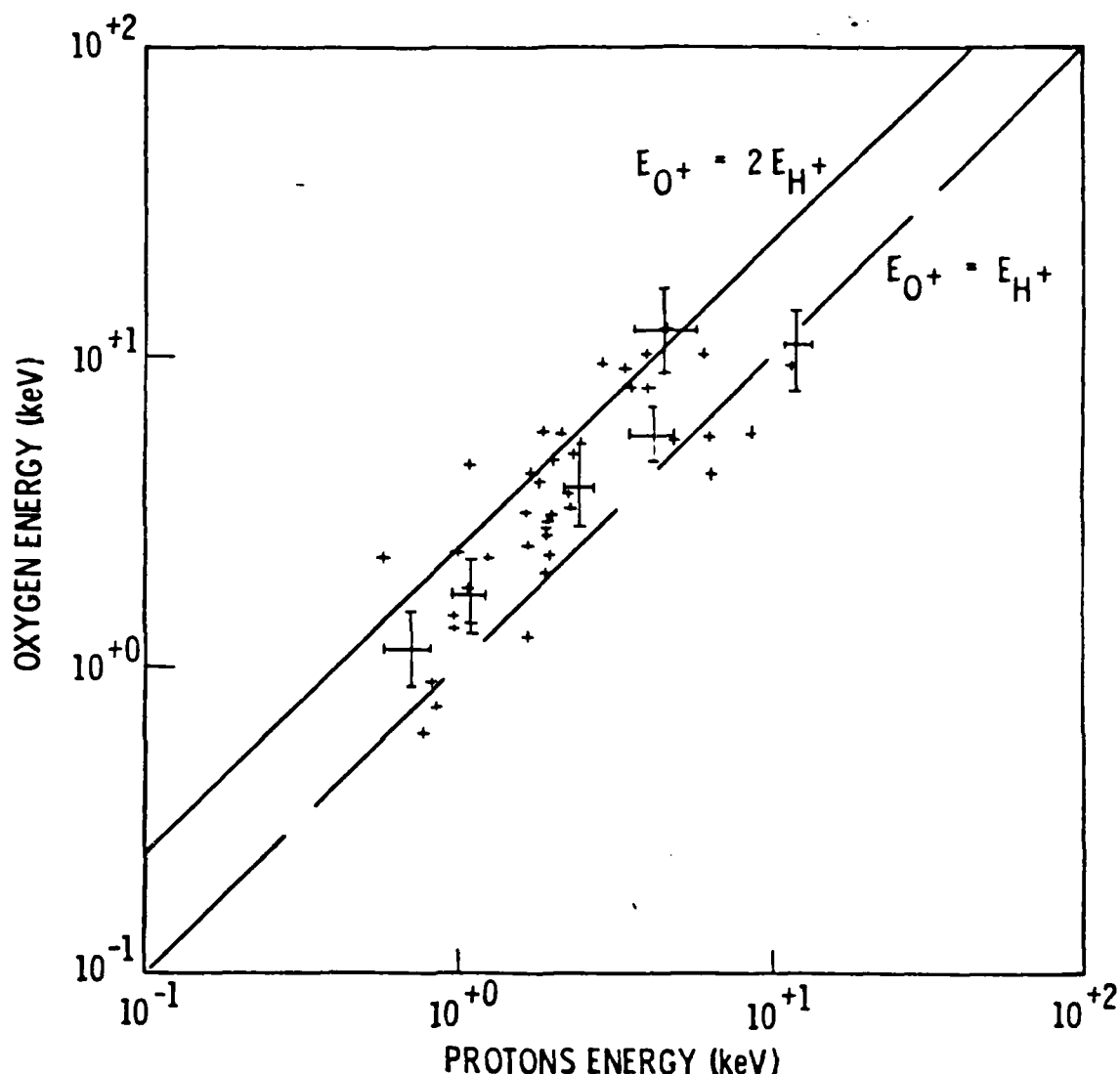
AVERAGE ENERGY OF UPFLOWING O^+ IONS VERSUS UPFLOWING H^+ IONS

Fig. 18. Scatter plot of the average energies of simultaneously observed upflowing O^+ and H^+ ions. The dashed line represents equal ion energies and the solid line represents O^+ energies twice that of H^+ . (COLLIN *et al.*, 1981).

discussed in Section 2 these results were taken to imply that the transverse acceleration mechanism responsible for the conical nature of the pitch angle distributions (the minimum along the field direction) preferentially acted on the O^+ ions and on average provided about half of their energy while the H^+ ions were primarily accelerated by a quasistatic parallel electric field.

In addition to the upflowing ion parameters, COLLIN *et al.* also recorded the characteristics of the trapped and precipitating energetic electrons ($0.07 \leq E \leq 24$ keV) on each spin in which upflowing ions were observed. Figure 20 shows a scatter plot of the oxygen ion energy versus the average energy of the trapped electrons (electron pitch angles between 80° and 100°). An equally good correlation was obtained with the

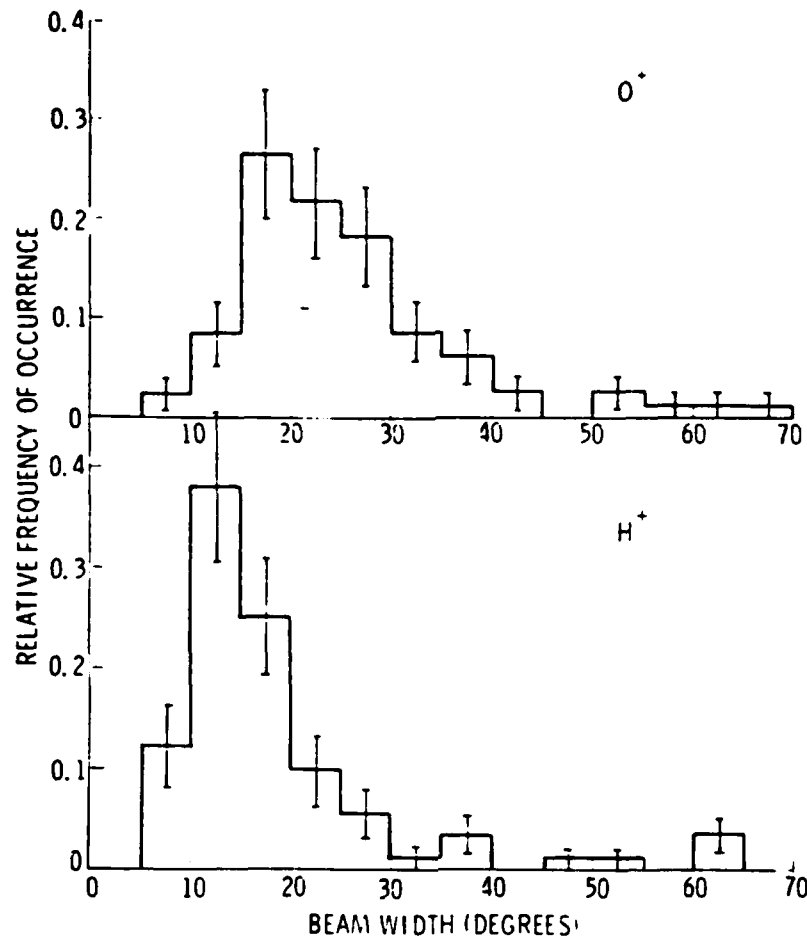


Fig. 19. Occurrence frequency distributions of beam half width at half maximum for upflowing O^+ and H^+ ions (COLLIN *et al.* 1981).

protons. The average electron energy was generally found to lie between the average proton energy and the average oxygen energy. A more detailed correspondence between the ions and electrons was apparent when the trapped electron data were sorted into 5 groups according to the average energy of the oxygen ion beam with which they were associated. Figure 21 shows the average differential electron energy spectrum for each group. A shoulder in the spectrum is apparent which moves to higher energies and develops into a peak as the ion energy increases. These results suggest that the electrons are also substantially energized by the electrostatic field that accelerates the ions and that the magnitude of their electrostatic acceleration is comparable to that of the ions. Thus statistically the \pm Edz above and below the 6,000 to 8,000 km altitude region of this study are approximately equal.

The results of a statistical study of some of the characteristics of the upward flowing O^+ ions accelerated in the low altitude dayside cusp were reported by SHELLEY (1979a). From 57 clearly identified cusp crossings on which S3-3 crossed 75° invariant latitude at an altitude above 5,000 km, upstreaming O^+ ion fluxes were detected in at least 58% of the cases. Conical distributions were approximately twice as frequently occurring as field aligned distributions. Because of energy and spatial limitations of the

AVERAGE TRAPPED ELECTRON ENERGY VERSUS AVERAGE O^+ ION ENERGY IN UPFLOWING ION EVENTS

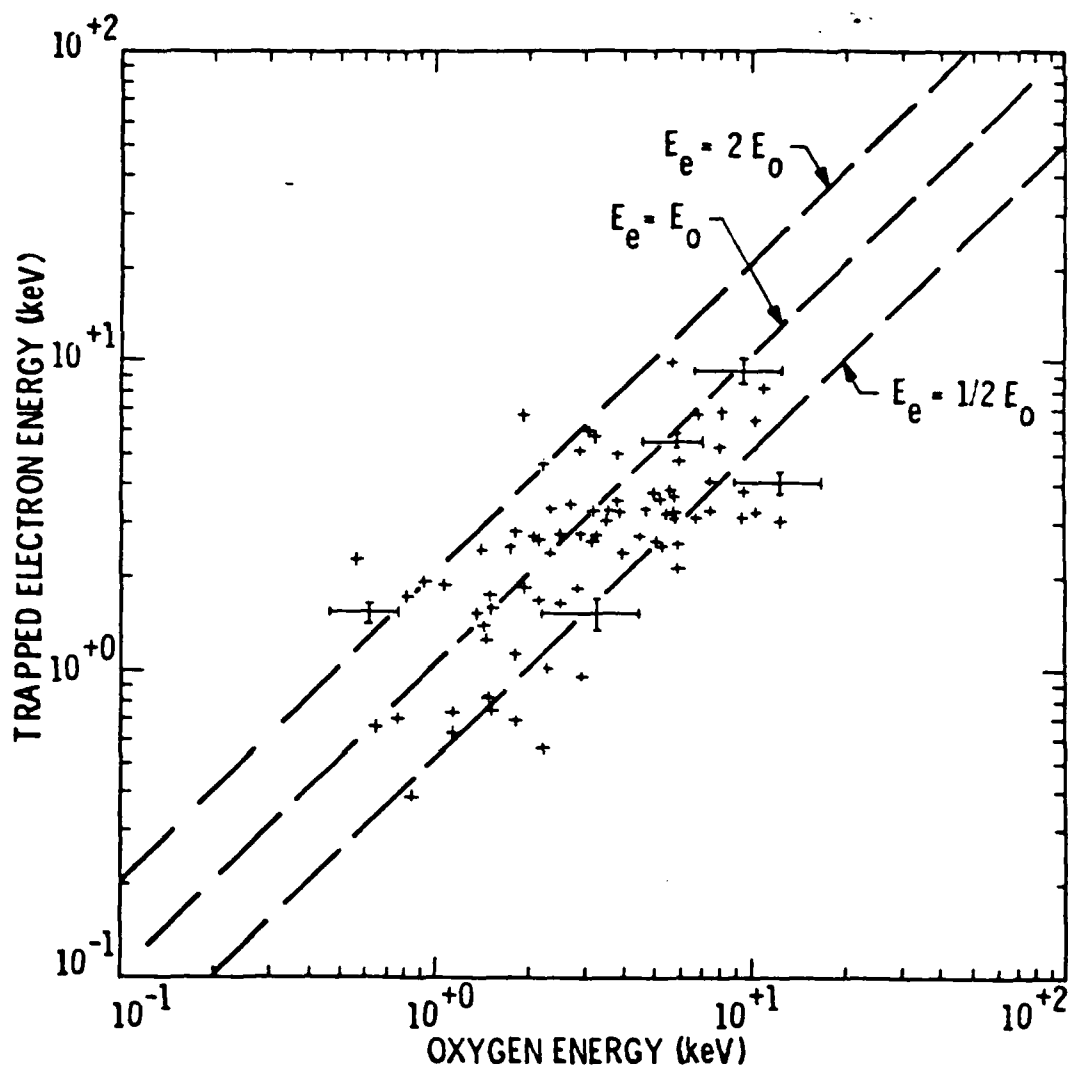


Fig. 20. Scatter plot of upflowing O^+ ion energy and average energy of electrons with pitch angles of $90^\circ \pm 10^\circ$. The dashed lines represent O^+ ion energies of twice, equal, and half the electron energies. (COLLIN *et al.*, 1981).

S3-3 experiment, the O^+ fluxes could easily have been missed on these traversals and so it was concluded that ionospheric ions are being accelerated in the cusp on a nearly continuous basis. These ions are injected into the boundary layer along with the plasma of solar wind origin which make up the bulk of the ion population in this region. They have been detected in the boundary layer or plasma mantle both in the subsolar regions (PETERSON *et al.*, 1981) and in the magnetotail (FRANK *et al.*, 1977). From the latter location they can be convected inward to the plasma sheet by the cross tail electric field and thereby enter the magnetospheric circulation system where they contribute to the ionospheric portion of this plasma population. (See SHARP *et al.* (1982) in this volume for further details of the ISEE-1 results.)

AVERAGE ELECTRON ENERGY SPECTRA AS A FUNCTION OF AVERAGE UPFLOWING O⁺ ION ENERGY

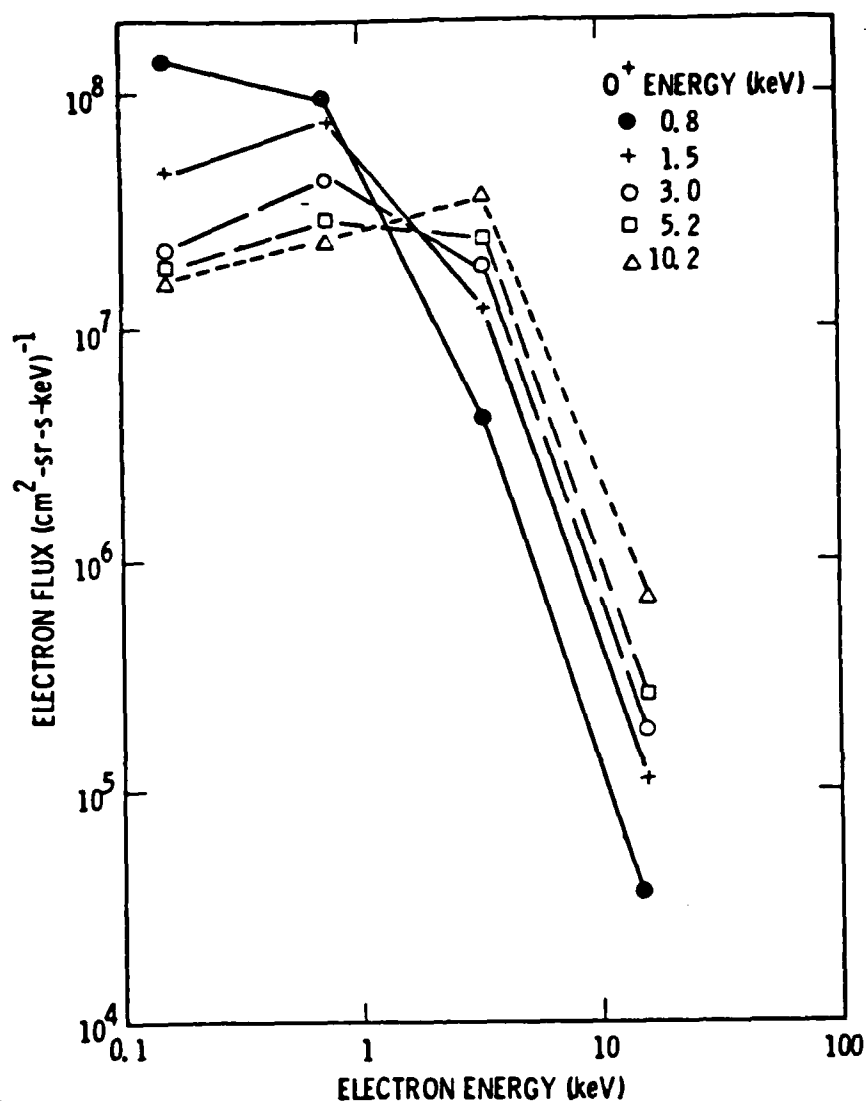


Fig. 21. Averaged differential electron energy spectrums for spins which were grouped according to the energy of the upflowing oxygen ions. (COLLIN *et al.*, 1981).

These statistical studies of the characteristics of the upward flowing ions have been supplemented in an important way by the results from the Aerospace Corporation electrostatic analyzer experiment on S3-3 (GORNEY *et al.*, 1981). Although lacking mass discrimination capabilities, this analyzer had higher sensitivity and covered a lower energy range (90 eV to 3.9 keV) and thereby was able to detect an important component of the upflowing ion population that was not accessible to the ion mass spectrometer. The statistical study reported by GORNEY *et al.* focussed on the significant differences in morphology between the ion distributions that had peak fluxes along the magnetic field direction (beams), and those with local minimums in that direction (conics). During quiet conditions ($K_p \leq 3$) the conical distributions were

found to show a local time distribution centered near noon, and a spatial association with the polar cusp, particularly for the events with $E < 400$ eV. The altitude distribution of these events was nearly uniform above an altitude of $\sim 2,000$ km. This contrasts with the results for the higher energy ions detected by the mass spectrometer and implies a low altitude generation region for these lower energy events. During disturbed times ($K_p > 3$) the conics were found to be relatively uniformly distributed in local time and their altitude distribution suggested a higher altitude generation region, particularly in the dusk sector. In contrast the ion beams observed during both quiet and disturbed times had a maximum occurrence frequency in the premidnight sector and were observed primarily in the 5,000–8,000 km altitude region in agreement with the characteristics of the more energetic ions detected by the mass spectrometer.

As discussed by GHIEMMETTI *et al.* (1978), GORNEY *et al.* (1981), and SHARP (1981), the ability to distinguish between beams and conics depends on a number of factors including: The angular resolution of the instrument; the altitude of the satellite relative to the acceleration region; and the minimum angle between the local magnetic field vector and the spin plane of the satellite. The Aerospace ion spectrometer had a field of view of $10^\circ \times 25^\circ$ (full width) while the Lockheed instrument subtended $6^\circ \times 5^\circ$. As mentioned above, COLLIN *et al.* found that a careful examination of the pitch angle distributions of upflowing ion events which were nominally classified as "beams" (events remaining after the obviously wide conics were sorted out) revealed numerous cases of angular distributions with local minimums along the field direction. They concluded that even the "beams", particularly the O^+ beams, have typically experienced a substantial transverse acceleration. GORNEY *et al.*'s results show that there is a class of low energy events with an even larger relative contribution from the transverse acceleration mechanism that exhibit a substantially different morphology than the other events.

3.5 Summary

To summarize the principal features of the morphology of the more energetic ($E > .5$ keV) upward flowing ion events, we found:

1. The average energies of the O^+ and H^+ beams were well correlated with each other and with the average energy of the electrons.
2. The flux intensities of O^+ and H^+ beams and the associated electrons did not show any significant correlations.
3. The O^+ beams were typically an order of magnitude less intense than the H^+ beams and about a factor of 1.5–2 more energetic.
4. A dramatic evening sector maximum in the occurrence frequency of the upflowing ions was observed which was not qualitatively different in quiet and disturbed times. The average energy of the peak upflowing ions was also substantially higher in this local time sector.
5. The composition of the upflowing ions was qualitatively different near local noon than in other local time sectors with O^+ conics dominating the observations.
6. The principal energization of the upflowing ions was shown to occur above 4,000 km and some evidence for a possible peak in the frequency of occurrence near 6,000 km altitude was presented.

7. The frequency of occurrence of the upflowing ions increased with increasing K_p , but there was no evidence of a change in the relative occurrence of O^+ and H^+ . The peak flux intensities of both H^+ and O^+ did not show a significant correlation with K_p . The mean and maximum energies of the ions increased with K_p , but there was no change in the O^+ relative to H^+ . These results do not exclude the possibility of a K_p dependence to the angular or energy widths of the ion distributions which might affect the total upward flow of ions. There is some limited evidence that the angular widths of the upflowing O^+ ions broadens with increasing ion energy while the H^+ cone widths narrow. [see figure 20 of SHELLEY (1979b).] Since the ion energy increases with increasing K_p , this suggests that there might in fact be an increase in the O^+/H^+ ratio during active times. More work is clearly required in this area.

4. Trapped Particles

The S3-3 spacecraft with apogee at $2.3 R_E$ provided the first opportunity to investigate the composition of the trapped hot plasmas in the radiation belts and particularly the composition of the inner ring current during geomagnetic storms. Although the trapped ions observed with S3-3 at high latitudes corresponded to equatorial pitch angles near the loss cone, the pitch angle measurements in the ring current below $L = 4$ typically corresponded to equatorial pitch angle ranges from 15° to 40° , and near the inner edge of the ring current, equatorial pitch angles as high as 50° were sampled (JOHNSON, *et al.*, 1977).

Prior to the S3-3 launch, observations of large fluxes of O^+ ions precipitating from the magnetosphere with energies up to 12 keV during magnetic storms had been reported from low altitude satellite measurements (SHELLEY *et al.*, 1972; SHARP, *et al.*, 1974; and JOHNSON, *et al.*, 1975). However, due to the spacecraft and spectrometer orientations, no measurements on the trapped component of the ion fluxes were obtained. Thus, direct injection and acceleration of the observed ions within or near the loss cone could not be excluded, although other considerations of the spatial and temporal distributions of the fluxes made it appear likely that significant fluxes of trapped ions were also present.

Using S3-3 data, JOHNSON *et al.* (1977) investigated the composition of the storm-time ring current during the early main phases of magnetic storms on 29 December 1976, 6 April 1977, and 19 April 1977 which had peak intensities near -100γ . From the mass spectrums shown for selected energies in Figure 22, it can be seen that O^+ and H^+ are the dominant ions observed although measurable amounts of He^+ are also observed. These data are from the L -shell range from about 3 to 4 and from the equatorial pitch angle range from 15° to 41° .

Energy spectrums of the O^+ and H^+ ions, corresponding to the data intervals of Figure 22, are shown in Figure 23. The high O^+ fluxes are evident, and the resulting O^+ number densities for these intervals in temporal order were 2.9, 3.3, and 7.1 with O^+/H^+ density ratios of 2.1, 3.0, and 1.5, respectively. Based on these high density ratios and in consideration of the low oxygen ion abundance in the solar wind (see BAME *et al.*, in this volume), it was concluded that the ionosphere was a major contributor to the storm-time ring current in the measured energy range.

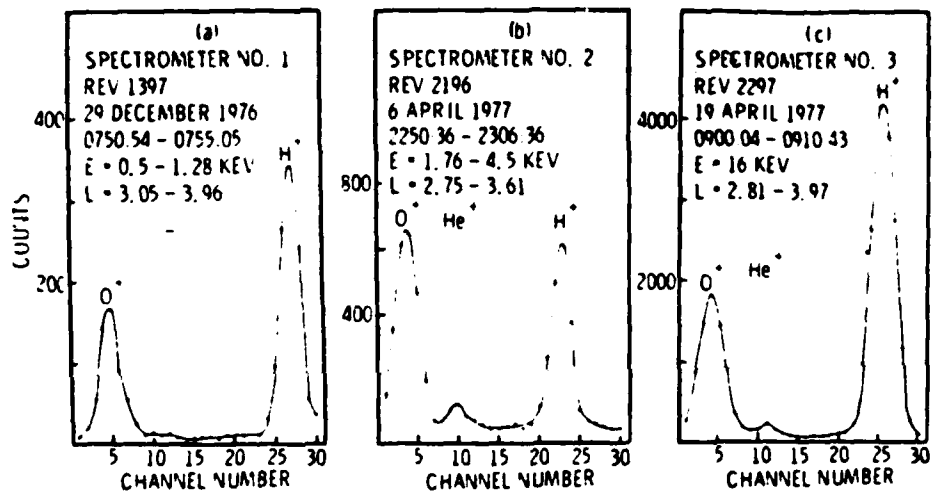


Fig. 22. Examples of mass spectrums from the three ion spectrometers during the main phases of the 29 December 1976, 6 April 1977, and 19 April 1977 magnetic storm (JOHNSON *et al.*, 1977).

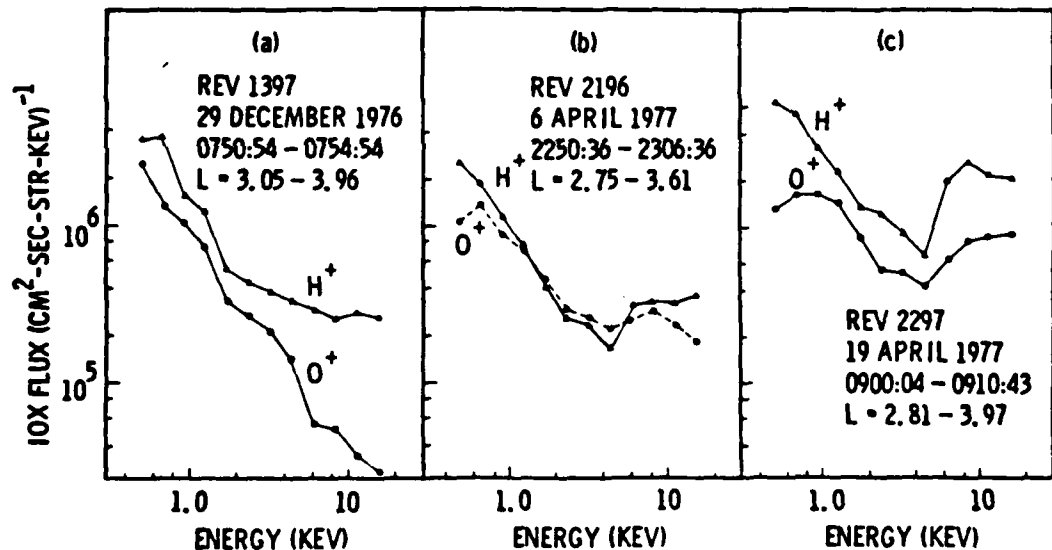


Fig. 23. Energy distributions for O^+ and H^+ during the main phases of the 29 December 1976, 6 April 1977, and 19 April 1977 magnetic storms. (JOHNSON *et al.*, 1977).

During the late recovery phase of the 29 December 1976 storm, the observed composition at low L -values was significantly different from that found during the main phase of the storm. As seen from the mass spectrum in Figure 24 (from JOHNSON, *et al.*, 1977) in comparison with the mass spectrums in Figure 22, there is an enhancement of He^+ and a depletion of H^+ relative to the O^+ . This temporal evolution in the ring current composition at low L -shells is *qualitatively* consistent with expectations based on the charge exchange loss process for the ion constituents (Tinsley [1976]; Lyons and Evans [1976]).

In addition to the charge exchange loss of ions from the ring current, as discussed above, evidence for a pitch angle scattering loss process for ring current ions has also

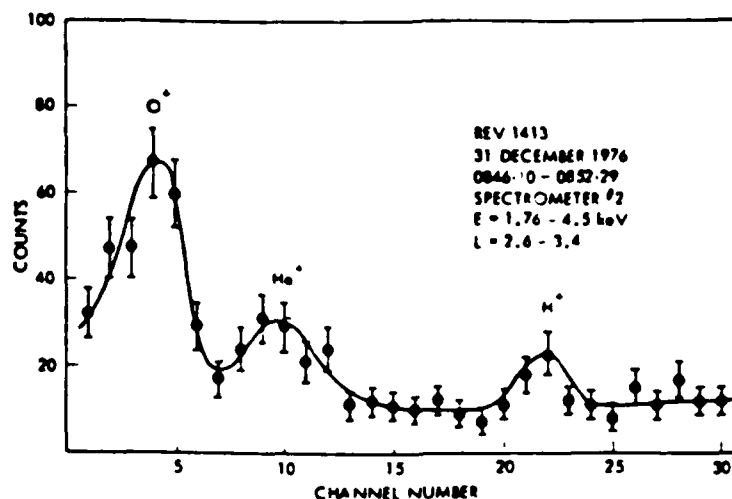


Fig. 24. An example of the mass spectrum during the recovery phase of the 29 December 1976 magnetic storm. (JOHNSON *et al.*, 1977).

been presented by JOHNSON *et al.* (1979). A segment of S3-3 data acquired during the main phase of the 11 December 1977 magnetic storm is shown in Figure 25. The abscissa shows universal time (SYST), longitude, latitude, altitude in kilometers, invariant latitude, and magnetic local time. The four lowest panels show electron spectrometer data (see JOHNSON *et al.*, 1979, for details of this format that are not discussed here). The panel labeled PITCH shows the pitch angle of the instrument look direction. The next four panels show the logarithm of the counts from ions with M/Q (mass/charge) = 1, 2, 4, and 16 summed once per second from the temporally selected output channels from each of the three mass spectrometers, giving an approximate measure of the relative flux of the relevant species. The next three panels (CXA-3, CXA-2, and CXA-1) display the mass spectrums accumulated at the selected energy step of each spectrometer. The selected energy step is given by the top panel with each spectrometer at its lowest energy for Step 1, etc. . The energy-per-unit-charge values are 0.5, 0.68, 0.94, and 1.28 keV for spectrometer #1; 1.76, 2.4, 3.3, and 4.5 keV for spectrometer #2; and 6.2, 8.5, 11.6, and 16.0 keV for spectrometer #3. The evidence for mass dependent pitch angle scattering can be seen by comparing the $M/Q = 1$ response, the $M/Q = 16$ response, and the pitch angle (PITCH) of the instrument look direction in the time period from 1200:22 to 1205:30. Loss cones for the H^+ ions in this region are generally well developed in both directions along the magnetic field; whereas, for the O^+ ions, the loss cone region near 0° pitch angle (the instrument pointed upward) contains high fluxes, and in some regions, nearly isotropic fluxes. From this event and other similar events, it is concluded that strong pitch angle scattering is occurring above the satellite for the O^+ ions, but not for H^+ ions. Thus, this loss process can contribute directly to the decay of the ring current by moving ions into the single transit loss cone. Possibly more important, even a slower rate of pitch angle scattering will continuously lower the mirror altitudes of the ions and thereby transport the ions into the denser region of the atmosphere where the charge exchange losses are more rapid. These observations of the mass dependence of the ion pitch angle

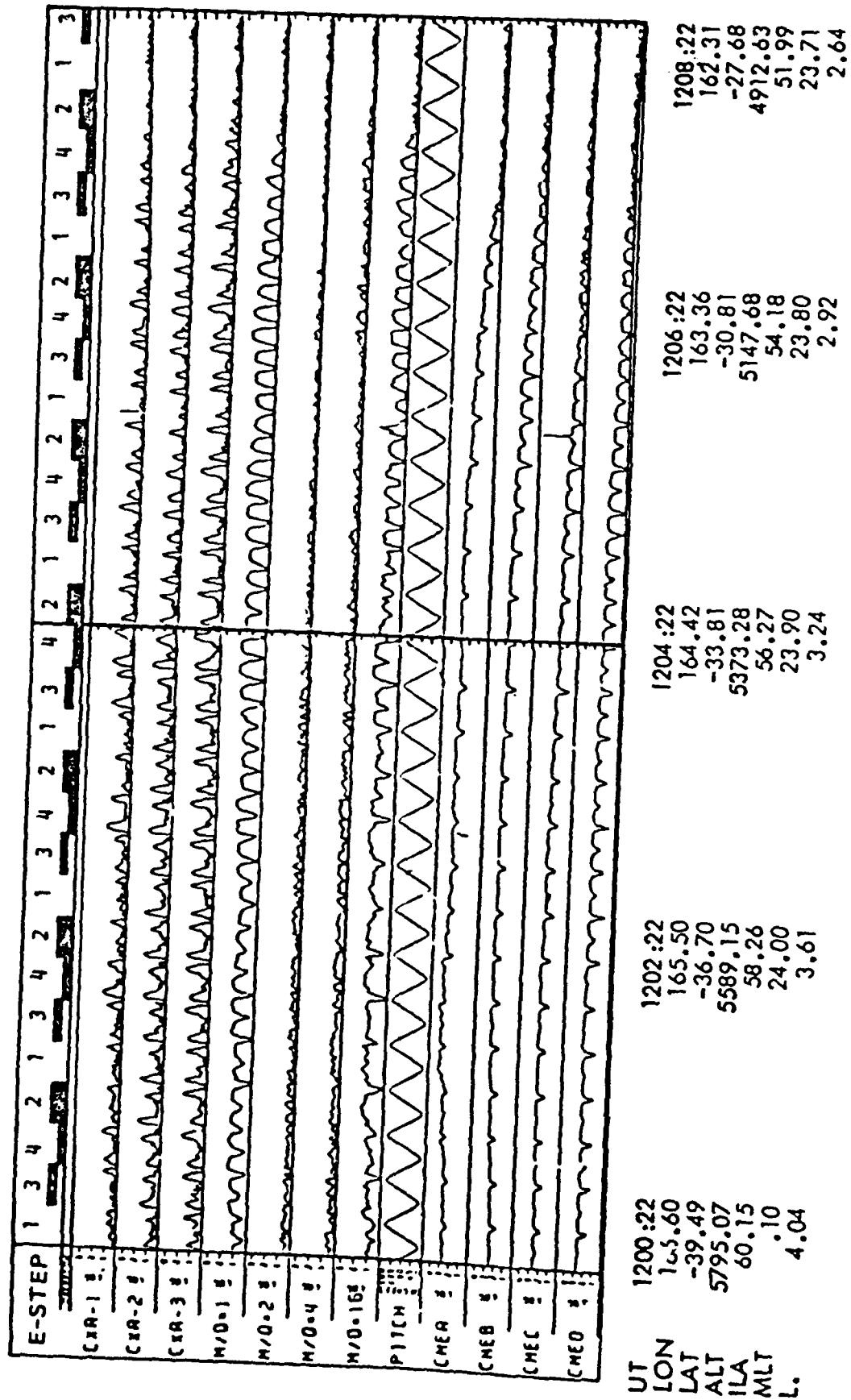


Fig. 25. Survey plot of S3-3 ion and electron data during the main phase of the 11 December 1977 magnetic storm. Large fluxes of precipitating O^+ ions are observed from 1200:22 to 1204:30 U.T. (JOHNSON *et al.*, 1979).

scattering rates, coupled with the spatial and/or temporal variations in these rates, suggested by the data in Figure 25, provide a further indication that quantitative modeling of the ring current decay by using only charge exchange loss processes may be applicable to only very limited regions of the magnetosphere and/or for limited geophysical conditions even in the equatorial regions of the magnetosphere.

5. Discussion

Since the launch of S3-3, a number of satellites carrying energetic ion mass spectrometers have been placed into high altitude orbits where they can sample the near equatorial trapped ion populations in the ring current and the distant plasma sheet (see reviews in this volume). As we see in these articles the results are complex and we do not yet have a clear understanding of the relative importance of the ion sources and the detailed operation of the dominant transport and loss mechanisms.

An important element of the puzzle is the morphology of the principal ionospheric source term, i.e. the composition and intensity, and the latitude, local time and magnetic activity dependence of the upward flowing energetic ions. (Other suggested ionospheric sources such as the plasmasphere and the polar wind have been shown to be of minor significance because of the general dominance of O^+ over He^+ in the trapped particle populations). The initial morphological results from S3-3 presented here are the best available information on the ionospheric source at this time.

As discussed by SHARP *et al.* (this volume) some of these results, e.g., the implied lack of dependence of the O^+/H^+ ratio on K_p , help us to understand the substorm associated changes in the composition of the distant plasma sheet. The principal process for removal of ions from that region is inward convection of the plasma with a velocity which is mass independent. One, therefore, would expect changes in the relative importance of the ionosphere and solar wind as source terms to be directly reflected by an increase in O^+ density as He^+ decreases and vice versa. This is indeed the case. The situation is apparently more complicated in the $L = 6$ to 11 region, where both O^+ and He^+ increase in the trapped population relative to H^+ during the early phase of large magnetic storms (LENNARTSSON, 1981). Possible explanations could be an increase in the O^+/H^+ ratio of the ionospheric source term, mass dependent losses, or both.

Figure 1 shows that almost all of the upward flowing ion events occurred at invariant latitudes above 66° ($L > 6$). These are the events for which the above described magnetic activity variations are pertinent. As we have seen, these results suggest that there was not an increase in the O^+/H^+ ratio with increasing K_p . However, the comparison of statistical results taken during different periods is subject to many uncertainties. There may be seasonal or long term (solar cycle) variations. Also, as discussed above, the study was based on peak flux intensities rather than the integral upflowing ion flux. Furthermore, K_p is not the ideal parameter to represent the early phase of magnetic storms. It is probably more relevant to substorm activity and therefore to the ISEE results in the distant plasma sheet where there is no apparent inconsistency.

As indicated above, another possibility is mass dependent loss terms. One expects

that charge exchange would be more important in the inner magnetosphere than in the distant plasma sheet but this gives the reverse effect to that which is observed. H^+ ions have the largest cross section for charge exchange in this energy range and should be depleted relative to the heavy ions in the trapped population. Thus during quiet times one would expect an increase in O^+ and He^{++} relative to H^+ , opposite to the observed trend in the $L > 6$ range. The expected trend is in fact observed at lower altitudes where the charge exchange mechanism is more important (JOHNSON *et al.*, 1977; LUNDIN *et al.*, 1980; LENNARTSSON, 1981).

Pitch angle diffusion into the loss cone is another significant loss process for ring current ions (SHARP *et al.*, 1977a) and there is evidence that at least on some occasions and in some locations in the magnetosphere this loss is enhanced for O^+ relative to H^+ . As we have seen in Figure 25, for invariant latitudes below about 60° the H^+ fluxes exhibit nearly empty loss cones both parallel and antiparallel to the magnetic field direction and appear to be relatively stably trapped while the O^+ pitch angle distributions show evidence for substantial pitch angle diffusion and subsequent precipitation. Unfortunately in the relevant range of $L > 6$ during quiet times the flux intensities are generally too low to see if this effect persists.

We would like to thank T. C. SANDERS, E. HERTZBERG, J. D. MATHEWS, J. D. MCDANIEL, L. HOOKER, and D. L. CARR for their important contributions to the S3-3 ion composition experiment and thus to the advances in space science resulting therefrom.

We also thank W. LENNARTSSON for his comments on the manuscript and R. WRIGHT for his assistance with the figures. This work has been supported by the Office of Naval Research under contract N00014-78-C-0479, the Atmospheric Sciences Section of the National Science Foundation under grant ATM-7911174, and NASA under contract NASW-3395.

REFERENCES

- CLADIS, J. B. and R. D. SHARP, Scale of electric field along magnetic field in an inverted V event, *J. Geophys. Res.*, **84**, 6564, 1979.
- COLLIN, H. L., R. D. SHARP, E. G. SHELLEY, and R. G. JOHNSON, Some general characteristics of upflowing ion beams over the auroral zone and their relationship to auroral electrons, *J. Geophys. Res.*, **86**, 6820, 1981.
- EVANS, D. S., Evidence for the low altitude acceleration of auroral particles in *Physics of the Hot Plasma in the Magnetosphere*, edited by B. HULTQVIST and L. STENFLO, Plenum Publishing Co., New York, 1975.
- FRANK, L. A., K. L. ACKERSON, and D. M. YEAGER, Observations of atomic oxygen (O^+) in the earth's magnetotail, *J. Geophys. Res.*, **82**, 129, 1977.
- GHIEMMETTI, A. G., Upward flowing ion characteristics in the high latitude ionospheric acceleration regions, (abstract), *EOS*, **59**, 1155, 1978.
- GHIEMMETTI, A. G., R. G. JOHNSON, R. D. SHARP, and E. G. SHELLEY, The latitudinal, diurnal, and altitudinal distributions of upward flowing energetic ions of ionospheric origin, *Geophys. Res. Lett.*, **5**, 59, 1978.
- GHIEMMETTI, A. G., R. D. SHARP, E. G. SHELLEY, and R. G. JOHNSON, Downward flowing ions and evidence for injection of ionospheric ions into the plasma sheet, *J. Geophys. Res.*, **84**, 5781, 1979.
- GORNEY, D. J., A. CLARKE, D. CROLEY, J. F. FENNELL, J. LUHMAN, and P. F. MIZERA, The distribution of ion beams and conics below 8,000 km, *J. Geophys. Res.*, **86**, 83, 1981.
- GURNETT, D. A., Electric field and plasma observations in the magnetosphere, in *Critical Problems of Magnetospheric Physics*, edited by E. R. DYER, National Academy of Sciences, Washington, D.C., 1972.

- JOHNSON, R. G., R. D. SHARP, and E. G. SHELLEY, Study of stormtime fluxes of heavy ions. Final report, NASA contract NASW-3112, LMSC/D673774, April 1979.
- JOHNSON, R. G., R. D. SHARP, and E. G. SHELLEY, Observations of ions of ionospheric origin in the stormtime ring current, *Geophys. Res. Lett.*, **4**, 403, 1977.
- JOHNSON, R. G., R. D. SHARP, and E. G. SHELLEY, Composition of the hot plasma in the magnetosphere, in *Physics of the hot plasma in the magnetosphere*, edited by B. HULTQVIST and L. STENFLO, Plenum, New York, 1975.
- LENNARTSSON, W., A comparison of the near equatorial ion composition between quiet and disturbed conditions, *J. Geophys. Res.*, **87**, 6109, 1982.
- LUNDIN, R., L. R. LYONS, and N. PISSARENKO, Observations of ring current composition at $L < 4$, *Geophys. Res. Lett.*, **7**, 425, 1980.
- LYONS, L. R. and D. S. EVANS, The inconsistency between proton charge exchange and the observed ring current decay, *J. Geophys. Res.*, **81**, 6197, 1976.
- MIZERA, P. F. and J. F. FENNELL, Signatures of electric fields from high and low altitude particle distributions, *Geophys. Res. Lett.*, **4**, 311, 1977.
- MIZERA, P. F., J. F. FENNELL, D. R. CROLEY, A. L. VAMPOLA, F. S. MOZER, R. B. TORBERT, M. TEMERIN, R. LYSAK, M. HUDSON, C. A. CATTELL, R. G. JOHNSON, R. D. SHARP, A. GHIEMMETTI, and P. M. KINTNER, The aurora inferred from S3-3 particles and fields, *J. Geophys. Res.*, **86**, 2329, 1981.
- MOZER, F. S., C. A. CATTELL, M. TEMERIN, R. B. TORBERT, S. VONGLINSKI, M. WOLDORFF, and J. WYGANT, The DC and AC electric field, plasma density, plasma temperature, and field-aligned current experiments on the S3-3 satellite, *J. Geophys. Res.*, **84**, 5875, 1979.
- PETERSON, W. K., E. G. SHELLEY, G. HAERENDEL, G. PASCHMANN, Energetic ion composition in the subsolar magnetopause and boundary layer, *J. Geophys. Res.*, **87**, 2139, 1982.
- SHARP, R. D., R. G. JOHNSON, E. G. SHELLEY, and K. K. HARRIS, Energetic O^+ ions in the magnetosphere, *J. Geophys. Res.*, **79**, 1844, 1974.
- SHARP, R. D., E. G. SHELLEY, and R. G. JOHNSON, A search for Helium ions in the recovery phase of a magnetic storm, *J. Geophys. Res.*, **82**, 2361, 1977a.
- SHARP, R. D., R. G. JOHNSON, and E. G. SHELLEY, Observations of an ionospheric acceleration mechanism producing energetic (keV) ions primarily normal to the geomagnetic field direction, *J. Geophys. Res.*, **82**, 3324, 1977b.
- SHARP, R. D., R. G. JOHNSON, and E. G. SHELLEY, Energetic particle measurements from within ionospheric structures responsible for auroral acceleration processes, *J. Geophys. Res.*, **84**, 480, 1979.
- SHARP, R. D., Positive ion acceleration in the $1 R_E$ altitude range, in *The Physics of Auroral Arc Formation*, edited by S. I. AKASOFU and J. R. KAN, Geophysical Monograph 25, American Geophysical Union, Washington, D.C., 1981, p. 112.
- SHELLEY, E. G., R. G. JOHNSON, and R. D. SHARP, Satellite observations of energetic heavy ions during a geomagnetic storm, *J. Geophys. Res.*, **77**, 6104, 1972.
- SHELLEY, E. G., R. D. SHARP, and R. G. JOHNSON, Satellite observations of an ionospheric acceleration mechanism, *Geophys. Res. Lett.*, **3**, 654, 1976.
- SHELLEY, E. G., Ion Composition in the dayside cusp: Injection of ionospheric ions into the high latitude boundary layer, Proceedings of Magnetospheric Boundary Layers Conference, Alpbach, 11-15 June, 1979 (ESA SP-148, August 1979a).
- SHELLEY, E. G., Heavy ions in the magnetosphere, *Space Science Reviews* **23**, 465, 1979b.
- SHELLEY, E. G., R. G. JOHNSON, and A. GHIEMMETTI, Relationship of upward flowing energetic ions to geomagnetic activity, (abstract), *EOS*, **61**, 1080, 1980.
- TINSLEY, B. A., Evidence that the recovery phase ring current consists of helium ions, *J. Geophys. Res.*, **81**, 6193, 1976.

END

FILMED

2-85

DTIC